

**Noname manuscript No.**  
(will be inserted by the editor)

# An Adaptive Second-order Method for a Class of Nonconvex Nonsmooth Composite Optimization

Hao wang · Xiangyu Yang · Yichen Zhu

Received: date / Accepted: date

**Abstract** This paper explores a specific type of nonconvex sparsity-promoting regularization problems, namely those involving  $\ell_p$ -norm regularization, in conjunction with a twice continuously differentiable loss function. We propose a novel second-order algorithm designed to effectively address this class of challenging nonconvex and nonsmooth problems, showcasing several innovative features: (i) The use of an alternating strategy to solve a reweighted  $\ell_1$  regularized subproblem and the subspace approximate Newton step. (ii) The reweighted  $\ell_1$  regularized subproblem relies on a convex approximation to the nonconvex regularization term, enabling a closed-form solution characterized by the soft-thresholding operator. This feature allows our method to be applied to various nonconvex regularization problems. (iii) Our algorithm ensures that the iterates maintain their sign values and that nonzero components are kept away from 0 for a sufficient number of iterations, eventually transitioning to a perturbed Newton method. (iv) We provide theoretical guarantees of global convergence, local superlinear convergence in the presence of the Kurdyka-Łojasiewicz (KL) property, and local quadratic convergence when employing the exact Newton step in our algorithm. We also showcase the effectiveness of our approach through experiments on a diverse set of model prediction problems.

**Keywords** nonconvex regularized optimization, subspace minimization, regularized Newton method, iteratively reweighted method

---

Hao wang  
ShanghaiTech University, Shanghai, China  
E-mail: haw309@gmail.com

Xiangyu Yang  
Henan University, Zhengzhou, China  
E-mail: yangxy@henu.edu.cn

Yichen Zhu  
ShanghaiTech University, Shanghai, China  
E-mail: zhuych2022@shanghaitech.edu.cn

## 1 Introduction

In this paper, we consider optimization problems of the form

$$\min_{\mathbf{x} \in \mathbb{R}^n} F(\mathbf{x}) := f(\mathbf{x}) + \lambda h(\mathbf{x}), \quad (1)$$

where  $f : \mathbb{R}^n \rightarrow \mathbb{R}$  is a twice continuously differentiable function but possibly nonconvex,  $\lambda > 0$  refers to the regularization parameter, and the regularization function  $h : \mathbb{R}^n \rightarrow [0, +\infty)$  is a sum of composite functions as follows

$$h(\mathbf{x}) := \sum_{i=1}^n (r \circ |\cdot|)(\mathbf{x}), \quad \forall \mathbf{x} \in \mathbb{R}^n. \quad (2)$$

The function  $f$  and  $r$  satisfy the following assumptions:

**Assumption 1** (i) *Throughout  $f$  is level-bounded [1, Definition 1.8].*  
(ii)  $r : [0, +\infty) \rightarrow [0, +\infty)$  is smooth on  $(0, +\infty)$  with  $r'(t) > 0$  and  $r''(t) \leq 0$  for  $t \in (0, +\infty)$ , and is subdifferentiable at 0. Moreover,  $r$  satisfies  $r(0) = 0$ ,  $r'(t)$  is convex,  $\lim_{t \rightarrow +\infty} r(t) = +\infty$  and  $\lim_{t \rightarrow +\infty} \frac{r'(t)}{t} = 0$  over  $t \in (0, +\infty)$ .

Assumption 1(i) implies that  $\lim_{\mathbf{x} \in \mathbb{R}^n : \|\mathbf{x}\| \rightarrow \infty} F(\mathbf{x}) = +\infty$  and further implies  $\min_{\mathbf{x} \in \mathbb{R}^n} F(\mathbf{x}) = \underline{F} > -\infty$  and  $\{\mathbf{x} \mid \operatorname{argmin}_{\mathbf{x} \in \mathbb{R}^n} F(\mathbf{x})\} \neq \emptyset$  regarding  $(\mathcal{P})$ . Assumption 1(ii) on the function  $r$  is sufficiently general, allowing (2) to cover several important instances of (1). Specifically, the function  $h$  can represent many proposed nonconvex regularization functions that enhance the sparsity of the desired solution, serving as efficient nonconvex surrogates for the  $\ell_0$  norm. Typical examples include the  $\ell_p$ -norm with  $p \in (0, 1)$  [2], Smoothly Clipped Absolute Deviation [3], Minimax Concave Penalty [4], and Capped  $\ell_1$  [5], to name just a few. Extensive computational research has shown that nonconvex regularization functions can effectively avoid solutions from biased solution spaces, unlike convex counterparts such as the  $\ell_1$ -norm. Moreover, [6] theoretically demonstrated that minimizing nonconvex regularizers requires significantly fewer measurements than traditional  $\ell_1$ -norm minimization. These advancements highlight the prevalence of composite optimization problems of the form (1) in applications such as sparse learning, model compression, compressive sensing, and signal and image processing (see, e.g., [7, 8, 9, 10]).

The nonconvex  $\ell_p$  norm, with  $p \in (0, 1)$ , is widely recognized as an efficient and effective regularizer for achieving desired sparse solutions, as supported by extensive research [11, 7, 8, 9, 10]. In addition,  $\ell_p$ -norm is a particular case of (2) where  $\lim_{t \rightarrow 0_+} (|t|_p^p)' = +\infty$ , which in principle makes it more challenging to solve compared to other nonconvex regularizers. Given these considerations, this paper mainly focuses on the  $p$ th power of the  $\ell_p$  norm regularization optimization problem:

$$\min_{\mathbf{x} \in \mathbb{R}^n} F(\mathbf{x}) := f(\mathbf{x}) + \lambda \|\mathbf{x}\|_p^p. \quad (\mathcal{P})$$

Over the past decade, composite optimization problems of this form have been studied extensively. In general, a variety of approximating methods have been developed to address Problem  $\mathcal{P}$ , as detailed in studies by Lu [12], Wang et al. [13][14][15], Lai [16], Chen [17] and others [18][19][20][21]. These methods tackle

the nonconvexity and nonsmoothness of  $\ell_p$ -term using different approximation  $\phi$ . For example,

$$\phi_1(x_i) = \max\{\mu, |x_i|^p\}, \quad \phi_2(x_i) = p(|x_i^k|^\alpha + \epsilon_i)^{\frac{p}{\alpha}-1} |x_i|^\alpha.$$

with  $\mu > 0, \alpha \geq 1, \epsilon \geq 0, \mathbf{x}^k$  being the current iterate.  $\phi_1$  was introduced by Lu et al. [12], who constructed a Lipschitz continuous approximation around zero.  $\phi_2$  is recognized as the iteratively reweighted  $\ell_1(\ell_2)$  method when  $\alpha = 1(\alpha = 2)$ . This approach constructs a convex approximation by employing weights derived from the linearization of the  $\ell_p$  norm at the current iterate, a strategy that has been extensively considered in many first order methods [16][13][14][15]. Wang et al. [13] proposed an iterative reweighted  $\ell_1$  method using iterative soft-thresholding update, the basic iterative step reads as follows:

$$\mathbf{x}^{k+1} \in \operatorname{argmin}_{\mathbf{x} \in \mathbb{R}^n} \left\{ \langle \nabla f(\mathbf{x}), \mathbf{x} \rangle + \frac{\alpha}{2} \|\mathbf{x} - \mathbf{x}^k\|^2 + \sum_{i=1}^n p(|x_i^k| + \epsilon_i)^{p-1} |x_i|^\alpha \right\},$$

where  $\alpha > 0$  is a constant relating to the Lipschitz constant of  $f$ . Moreover, significant advancements have been made by Yu [22] and Wang et al. [15] by incorporating the extrapolation technique into the iteratively reweighted  $\ell_1$  methods. These authors established convergence results concerning perturbations under the Kurdyka-Łojasiewicz (KL) property. Chen [17] introduced a second-order method utilizing a smoothing trust region Newton approach for Problem 1, which approximates the regularizer with a twice continuously differentiable function. This method tackles the nonsmoothness of the  $|\cdot|$  operator using an iterative reweighted  $\ell_2$  approximation and demonstrates global convergence to a local minimizer. In these methods, the perturbation  $\epsilon$  plays a crucial role in the design of algorithms and in achieving convergence results. Wang et al. [13] developed a dynamic updating strategy that drives the perturbation associated with nonzero components towards zero while maintaining the others as constants. For  $p = \frac{1}{2}$  and  $\frac{2}{3}$ , the proximal gradient method is extensively used. Xu [20] provides a closed-form proximal mapping for these specific values of  $p$ . Although exact and inexact numerical methods for generic  $\ell_p$  proximal mapping have been proposed [23, 24], these methods are considerably slower than the closed-form solution and may sometimes be considered unaffordable for large-scale problems. Several first-order methods that capitalize on these developments have been introduced in recent works [11][25].

Second-order methods have focused extensively on general nonconvex and nonsmooth composite problems. Inspired by proximal mapping, a class of proximal Newton methods has emerged [26][27][28][29]. These methods require regularizer to be convex and solve the regularized proximal Newton problem globally, achieving a superlinear convergence rate under various assumptions (metric  $q(> 1/2)$ -subregularity assumption for [28], Luo-Tseng error Bound for [27], KL property for [29]).

Considering the specific sparsity-driven Problem 1, it exhibits a nature where the nonsmooth regularization functions usually present a smooth substructure, involving active manifolds where the functions are locally smooth. For instance, in Problem  $\mathcal{P}$ , the function is smooth around any point strictly bounded away from zero. Although  $\mathbf{x} = 0$  is a natural stationary point of  $F$  (see 8 for the stationarity condition), it is not a desirable solution in terms of objective value. Therefore, identifying an appropriate active manifold becomes a critical step in addressing

these problems. The proximal gradient method and its variants have proven effective in reaching the optimal submanifold [30][31]. The manifold identification complexity of different variants of the proximal gradient method is detailed in [32]. The iteratively reweighted method shares similar properties with the proximal gradient method, as their iterative forms and optimal conditions align (see 13). From this perspective, we have designed an automatic active manifold identification process using the iteratively reweighted method. After identifying a relatively optimal active manifold, transitioning to a Newton method is a logical step, as it is widely recognized that first-order methods are fast for global convergence but slow for local convergence. Employing a Newton method on the smooth active manifold typically yields a superlinear convergence rate. A class of hybrid methods for nonconvex and nonsmooth composite problems has been explored, utilizing a forward-backward envelope approach that integrates proximal gradient with Newton method [33][34][35]. However, few second-order methods specifically tailored for Problem  $\mathcal{P}$  have been proposed until recently. Wu et al. [36] introduced a hybrid approach combining the proximal gradient method with the subspace regularized Newton method, demonstrated to achieve a superlinear convergence rate under the framework of the Kurdyka-Łojasiewicz theory.

In this paper, we design and analyze second-order methods for the  $\ell_p$ -norm regularization problem (Problem  $\mathcal{P}$ ), which are also applicable to general nonconvex and nonsmooth regularization problems (Problem 1). Our method is a hybrid approach that alternates between solving an iteratively reweighted  $\ell_1$  subproblem and a subspace Newton subproblem. This hybrid framework integrates the subspace Newton method with a subspace iterative soft-thresholding technique, employing an approximate solution for the Newton subproblem to enhance algorithmic speed. Unlike proximal-type methods, each iteration of our method approximates the  $\ell_p$ -norm with a weighted  $\ell_1$ -norm and locally accelerates the process using the Newton direction, which enabling our method to solve for generic  $p$  ( $0 < p < 1$ ).

The adaptability of the Newton subproblem allows our method to incorporate various types of quadratic programming (QP) subproblems, achieving diverse convergence outcomes based on the subsolver employed. The proposed method achieves global convergence under the conditions of Lipschitz continuity of the function  $f$  and boundedness of the Hessian. Locally, we establish the convergence rate under the Kurdyka-Łojasiewicz (KL) property of  $F$  with different exponents, achieving superlinear convergence with an exponent of 1/2. By employing a strategic perturbation setting, we attain local quadratic convergence under the local Hessian Lipschitz continuity of  $F$  on the support. When extending our method to tackle the generic problems (Problem 1), the same convergence results are maintained.

Numerical experiments for Problem  $\mathcal{P}$  demonstrate the superior performance of our approach compared to existing methods, such as a hybrid method combining the proximal gradient and regularized Newton methods [36], and an extrapolated iteratively reweighted  $\ell_1$  method [15]. Our method shows notable advantages in time efficiency while maintaining comparable solution quality against existing first-order and second-order methods. Additional experiments on various regularization fitting problems (Problem 1) validate our algorithm's effectiveness across different settings.

Our work presents several distinguishing features compared to existing second-order methods. Unlike the smoothing trust region Newton method [17], which

requires a twice continuously differentiable approximation for regularization terms, our method uses a nonsmooth local model that retains the form of weighted  $\ell_1$  regularization and optimizes within a subspace, potentially yielding more efficient and targeted search directions. Moreover, our method dynamically identifies and exploits the active manifold during the optimization process, a feature not present in the smoothing trust region Newton method. Furthermore, unlike the hybrid method of proximal gradient and regularized Newton methods (HpgSRN) [36], which uses a proximal gradient method across the entire space to identify the active manifold, our method applies iterative soft thresholding updates on the subspaces of zero and nonzero components separately, enhancing and clarifying the identification process. This distinct approach allows our method to adopt an iteratively reweighted  $\ell_1$  structure globally and shift to the original problem locally.

### 1.1 Organization

The rest of this paper is organized as follows. §2 includes notation and the characterization of stationarity condition for the problem. §3 presents the algorithm and explain the design logic. §4 provides the global and local convergence analysis of our algorithm. §5 provides another local subproblem for our algorithm and extends our algorithm to generic nonconvex and nonsmooth sparsity-driven regularization problems. §6 shows the numerical experiments on the logistic regression problem.

## 2 Notation and Stationary Conditions

### 2.1 Notation

Throughout the paper, let  $\mathbb{R}^n$  denote the  $n$ -dimensional Euclidean space, equipped with the standard inner product  $\langle \cdot, \cdot \rangle$  and its induced norm  $\|\cdot\|$ . Let  $\mathbb{R}_{++}^n = \{\mathbf{x} \in \mathbb{R}^n \mid x_i > 0\}$ . For any  $\mathbf{x} \in \mathbb{R}^n$ , we use  $x_i$  to denote its  $i$ th component. For any symmetric matrix  $M \in \mathbb{R}^{n \times n}$ , define  $M_{\mathcal{I}}$  as the submatrix of  $M$  with rows and columns indexed by  $\mathcal{I}$ . Denote  $\mathbb{R}^{\mathcal{I}}$  the subspace consisting of the variables in  $\mathcal{I}$  and setting the rest as zero, i.e.,

$$\mathbb{R}^{\mathcal{I}} := \{\mathbf{x} \in \mathbb{R}^n \mid x_i = 0, i \in \mathcal{I}^c\}.$$

For a nonempty set  $\mathcal{S}$ , let  $|\mathcal{S}|$  denote its cardinality. Define  $[n] = \{1, 2, 3, \dots, n\}$ . Let  $\text{sgn}(x_i) = 1$  if  $x_i > 0$ ,  $\text{sgn}(x_i) = -1$  if  $x_i < 0$  and  $\text{sgn}(x_i) = 0$  if  $x_i = 0$ . Define the set of nonzeros and zeros of  $\mathbf{x}$  as

$$\mathcal{I}(\mathbf{x}) = \{i \mid x_i \neq 0\} \quad \text{and} \quad \mathcal{I}_0(\mathbf{x}) = \{i \mid x_i = 0\},$$

respectively.  $\mathcal{I}(\mathbf{x})$  is also known as the support of  $\mathbf{x}$ , and is further partitioned into  $\mathcal{I}(\mathbf{x}) = \mathcal{I}_+(\mathbf{x}) \cup \mathcal{I}_-(\mathbf{x})$  where

$$\mathcal{I}_+(\mathbf{x}) = \{i \mid x_i > 0\} \quad \text{and} \quad \mathcal{I}_-(\mathbf{x}) = \{i \mid x_i < 0\}.$$

Given  $\mathbf{v} \in \mathbb{R}^n$  and  $\boldsymbol{\omega} \in \mathbb{R}_{++}^n$ , the weighted soft-thresholding operator is defined as

$$[\mathbb{S}_{\boldsymbol{\omega}}(\mathbf{v})]_i := \text{sgn}(v_i) \max(|v_i| - \omega_i, 0).$$

For any  $\mathbf{x}, \mathbf{y} \in \mathbb{R}^n$ , let  $\mathbf{x} \circ \mathbf{y}$  denote the component-wise product of  $\mathbf{x}$  and  $\mathbf{y}$ , i.e.,  $[\mathbf{x} \circ \mathbf{y}]_i = x_i y_i$ ,  $\forall i \in [n]$ , and we use  $\mathbf{x} \leq \mathbf{y}$  to denote  $x_i \leq y_i$ ,  $\forall i \in [n]$ .

In  $\mathbb{R}^n$ , let  $\|\mathbf{x}\|$  denote the Euclidean norm of  $\mathbf{x}$  and the  $\|\mathbf{x}\|_p := (\sum_{i=1}^n |x_i|^p)^{\frac{1}{p}}$  denotes the  $\ell_p$  norm of  $\mathbf{x}$  (it is a norm if  $p \geq 1$  and a quasi-norm if  $0 < p < 1$ ). If function  $f : \mathbb{R}^n \rightarrow \mathbb{R} \cup \{+\infty\}$  is convex, then the subdifferential of  $f$  at  $\bar{\mathbf{x}}$  is given by

$$\partial f(\bar{\mathbf{x}}) := \{\mathbf{z} | f(\bar{\mathbf{x}}) + \langle \mathbf{z}, \mathbf{x} - \bar{\mathbf{x}} \rangle \leq f(\mathbf{x}), \forall \mathbf{x} \in \mathbb{R}^n\}.$$

If function  $f$  is lower semi-continuous, then the Frechet subdifferential of  $f$  at  $\mathbf{a}$  is given by

$$\partial_F f(\mathbf{a}) := \{\mathbf{z} \in \mathbb{R}^n | \liminf_{\mathbf{x} \rightarrow \mathbf{a}} \frac{f(\mathbf{x}) - f(\mathbf{a}) - \langle \mathbf{z}, \mathbf{x} - \mathbf{a} \rangle}{\|\mathbf{x} - \mathbf{a}\|_2} \geq 0\}$$

and the limiting subdifferential of  $f$  at  $\mathbf{a}$  is given by

$$\bar{\partial} f(\mathbf{a}) := \{\mathbf{z}^* = \lim_{\mathbf{x}^k \rightarrow \mathbf{a}, f(\mathbf{x}^k) \rightarrow f(\mathbf{a})} z^k, z^k \in \partial_F f(\mathbf{x}^k)\}.$$

We abuse our notation by writing  $\nabla_i F(\mathbf{x}) = \nabla_{x_i} F(\mathbf{x}) = \frac{\partial}{\partial x_i} F(\mathbf{x})$  if  $F$  is (partially) differentiable with respect to  $x_i$ ; we do not suggest  $\nabla_i F(\mathbf{x}) = [\nabla F(\mathbf{x})]_i$  since  $F$  may not be differentiable at  $\mathbf{x}$ . In addition, if  $F$  is differentiable with respect to a set of variables  $x_i, i \in \mathcal{I}$ ,  $\nabla_{\mathcal{I}} F(\mathbf{x})$  and  $\nabla_{x_{\mathcal{I}}} F(\mathbf{x})$  is the gradient subvector of  $\nabla_i F(\mathbf{x}), i \in \mathcal{I}$ . Also denote  $\nabla_{\mathcal{I}\mathcal{I}} F(\mathbf{x})$  as the subspace Hessian of  $F$  with respect to  $\mathcal{I}$  if  $F$  is (partially) smooth of  $x_i, \mathcal{I}$ .

$\mathbb{P}(\mathbf{y}; \mathbf{x})$  is defined to project a given vector  $\mathbf{y} \in \mathbb{R}^n$  onto the subspace containing  $\mathbf{x} \in \mathbb{R}^n$ , i.e.,

$$[\mathbb{P}(\mathbf{y}; \mathbf{x})]_i := \begin{cases} \max\{0, y_i\}, & \text{if } \mathcal{I}_+(\mathbf{x}), \\ \min\{0, y_i\}, & \text{if } \mathcal{I}_-(\mathbf{x}), \\ 0, & \text{if } \mathcal{I}_0(\mathbf{x}). \end{cases} \quad (3)$$

## 2.2 First-order stationary condition of (4)

We first recall the notion of first-order stationary points of  $(\mathcal{P})$ .

**Definition 1 (Stationary point [12, Definition 1])** We say that an  $\mathbf{x}^* \in \mathbb{R}^n$  is a first-stationary point of  $(\mathcal{P})$  if

$$x_i^* \nabla_i f(\mathbf{x}^*) + \lambda p |x_i^*|^p = 0, \quad \forall i \in [n]. \quad (4)$$

Or equivalently,

$$\nabla_i f(\mathbf{x}^*) + \lambda p |x_i^*|^{p-1} \text{sgn}(x_i^*) = 0, \quad \forall i \in \mathcal{I}(\mathbf{x}^*). \quad (5)$$

The following result is adapted from [12] and states that any local minimizer of  $(\mathcal{P})$  is a stationary point.

**Proposition 1** Consider  $(\mathcal{P})$  and let  $\mathbf{x}^*$  be a locally optimal solution. Then  $\mathbf{x}^*$  is a first-order stationary point, implying that (4) is satisfied at  $\mathbf{x}^*$ .

*Remark 1* By (5), we understand that solving for a first-order stationary solution involves identifying its support set. In other words, once the support of the stationary solutions is exactly determined, problem  $(\mathcal{P})$  transforms into a smooth optimization problem.

Next, we present the first-order stationary conditions of an approximation problem of  $(\mathcal{P})$ , which is the basis of the proposed algorithm. To overcome the nonsmoothness and non-Lipschitz continuity of  $\|\mathbf{x}\|_p$  at some  $x_i = 0$ ,  $\forall i \in [n]$ , we introduce a perturbation parameter  $\boldsymbol{\epsilon} \in \mathbb{R}_{++}^n$  to the  $\ell_p$  regularization term. This modification results in a smooth and locally Lipschitz continuous objective function, which reads

$$\min_{\mathbf{x} \in \mathbb{R}^n} F(\mathbf{x}; \boldsymbol{\epsilon}) := f(\mathbf{x}) + \lambda \sum_{i=1}^n (|x_i| + \epsilon_i)^p \quad (6)$$

with  $\epsilon_i > 0$ ,  $\forall i \in [n]$ . It is obvious that  $F(\mathbf{x}) = F(\mathbf{x}; \mathbf{0})$ . By [1, Theorem 10.1 & Exercise 8.8(c)], similar to Definition 1, we say that an  $\hat{\mathbf{x}} \in \mathbb{R}^n$  is a first-order stationary point of (6) if

$$0 \in \nabla_i f(\hat{\mathbf{x}}) + \omega_i \partial |\hat{x}_i|, \quad \forall i \in [n], \quad (7)$$

where  $\omega_i := \omega(\hat{x}_i, \epsilon_i) = \lambda p (|\hat{x}_i| + \epsilon_i)^{p-1}$ ,  $\forall i \in [n]$ . An equivalent form of (7) can be written as

$$\begin{aligned} |\nabla_i f(\hat{\mathbf{x}})| &\leq \omega_i, & i \in \mathcal{I}_0(\hat{\mathbf{x}}), \\ \nabla_i f(\hat{\mathbf{x}}) + \omega_i \text{sgn}(\hat{x}_i) &= 0, & i \in \mathcal{I}(\hat{\mathbf{x}}). \end{aligned} \quad (8)$$

The following relationship is revealed between (5) and (7) at  $\mathbf{x}$ . That is,

$$(7) \text{ holds at } \mathbf{x} \text{ and } \epsilon_i = 0, i \in \mathcal{I}(\mathbf{x}) \iff (5) \text{ holds at } \mathbf{x}. \quad (9)$$

### 3 Proposed SOIR $\ell_1$

In this section, we present the proposed second-order iteratively reweighted  $\ell_1$  algorithm for solving  $(\mathcal{P})$ , hereafter referred to SOIR $\ell_1$ , as stated in Algorithm 1. SOIR $\ell_1$  incorporates ideas of subspace acceleration and support identification. It alternates between minimization in a reduced space—determined by the stationarity measures of the zeros and nonzeros in the current solution estimate—and implements iterative soft-thresholding (IST) step during the alternating optimization. The IST step serves both to identify the support of an optimal solution and to ensure the algorithm’s convergence. Whenever the signs of the two successive iterates remain unchanged during iteration, we switch the IST step to an inexact subspace regularized Newton step to enhance convergence. Once the optimal support is identified, SOIR $\ell_1$  then implements a second-order method solely over the nonzeros variables in the support.

**Algorithm 1** Proposed SOIR $\ell_1$  for solving  $(\mathcal{P})$ 


---

**Require:**  $(\mathbf{x}^0, \boldsymbol{\epsilon}^0) \in \mathbb{R}^n \times \mathbb{R}_{++}^n$ ,  $\{\eta_\Phi, \eta_\Psi\} \in (0, 1]$ ,  $\{\beta, \xi\} \in (0, 1)$ ,  $\{\bar{\mu}, \gamma, \tau, \alpha, \zeta_0\} \in (0, \infty)$  and  $\varpi \in (0, 1/2]$ .

- 1: **for**  $k = 0, 1, 2, \dots$  **do**
- 2:   **while**  $\max\{\|\Psi(\mathbf{x}^k; \boldsymbol{\epsilon}^k)\|, \|\Phi(\mathbf{x}^k; \boldsymbol{\epsilon}^k)\|\} \leq \tau$  **do**
- 3:     **if**  $\epsilon_i^k \leq \tau, i \in \mathcal{I}^k$  **then**
- 4:       **return** the (approximate) solution  $\mathbf{x}^k$  of problem  $(\mathcal{P})$ .
- 5:     **else**
- 6:       Set  $\epsilon_i^k \in (0, \beta \epsilon_i^k)$ ,  $i \in \mathcal{I}^k$ .
- 7:     **end if**
- 8:   **end while**
- 9:   **if**  $\|\Psi(\mathbf{x}^k; \boldsymbol{\epsilon}^k)\| \geq \gamma \|\Phi(\mathbf{x}^k; \boldsymbol{\epsilon}^k)\|$  **then**
- 10:     Choose  $\mathcal{W}_k \subseteq \{i : [\Psi(\mathbf{x}^k; \boldsymbol{\epsilon}^k)]_i \neq 0\}$  such that  $\|[\Psi(\mathbf{x}^k; \boldsymbol{\epsilon}^k)]_{\mathcal{W}_k}\| \geq \eta_\Psi \|\Psi(\mathbf{x}^k; \boldsymbol{\epsilon}^k)\|$ .
- 11:     Call Algorithm 2 to compute  $(\mathbf{x}^{k+1}, \mu^k) \leftarrow \text{IST}(\mathbf{x}^k, \omega^k, \mathcal{W}_k; \alpha, \xi, \bar{\mu})$ .
- 12:   **else**
- 13:     Choose  $\mathcal{W}_k \subseteq \{i : [\Phi(\mathbf{x}^k; \boldsymbol{\epsilon}^k)]_i \neq 0\}$  such that  $\|[\Phi(\mathbf{x}^k; \boldsymbol{\epsilon}^k)]_{\mathcal{W}_k}\| \geq \eta_\Phi \|\Phi(\mathbf{x}^k; \boldsymbol{\epsilon}^k)\|$ .
- 14:     Call Algorithm 2 to compute  $(\hat{\mathbf{x}}^{k+1}, \mu_k) \leftarrow \text{IST}(\mathbf{x}^k, \omega^k, \mathcal{W}_k; \alpha, \xi, \bar{\mu})$ .
- 15:     **if**  $\text{sgn}(\hat{\mathbf{x}}^{k+1}) = \text{sgn}(\mathbf{x}^k)$  **then**
- 16:       Set  $\mathbf{H}^k \leftarrow \nabla_{\mathcal{W}_k \mathcal{W}_k}^2 F(\mathbf{x}^k; \boldsymbol{\epsilon}^k) + \zeta_k \mathbf{I} \succ \mathbf{0}$  and  $\mathbf{g}^k \leftarrow \nabla_{\mathcal{W}_k} F(\mathbf{x}^k; \boldsymbol{\epsilon}^k)$ .
- 17:       Compute a reference direction  $\mathbf{d}_R^k \leftarrow -\frac{\|\mathbf{g}^k\|^2}{\langle \mathbf{g}^k, \mathbf{H}^k \mathbf{g}^k \rangle} \mathbf{g}^k$ .
- 18:       Compute any
- 19:       
$$\bar{\mathbf{d}}^k \approx \text{argmin}_{\mathbf{d}} \langle \mathbf{g}^k, \mathbf{d} \rangle + \frac{1}{2} \langle \mathbf{d}^k, \mathbf{H}^k \mathbf{d}^k \rangle,$$

such that

$$\langle \mathbf{g}^k, \bar{\mathbf{d}}^k \rangle \leq \langle \mathbf{g}^k, \mathbf{d}_R^k \rangle \text{ and } m_k(\bar{\mathbf{d}}^k) \leq m_k(\mathbf{0}). \quad (10)$$
- 20:       Set  $\mathbf{d}_{\mathcal{W}_k}^k = \bar{\mathbf{d}}^k$ ,  $\mathbf{d}_{\mathcal{W}_k^c}^k = \mathbf{0}$ .
- 21:       Call Algorithm 3 to compute  $(\mathbf{x}^{k+1}, \mu^k) \leftarrow \text{PLS}(\mathbf{x}^k; \boldsymbol{\epsilon}^k, \mathbf{d}^k, \mathcal{W}_k; \varpi, \xi)$ .
- 22:     **else**
- 23:       Set  $\mathbf{x}^{k+1} \leftarrow \hat{\mathbf{x}}^{k+1}$ .
- 24:     **end if**
- 25:     Update  $\epsilon_i^{k+1} \in (0, \beta \epsilon_i^k)$ ,  $i \in \mathcal{I}^{k+1}$ .
- 26:     Update  $\omega_i^{k+1} = \lambda p(|x_i^{k+1}| + \epsilon_i^{k+1})^{p-1}$ ,  $i \in [n]$ .
- 27: **end for**

---

3.1 Local Weighted  $\ell_1$  Regularized Models and Stationarity Measures

Our approach for solving  $(\mathcal{P})$  is partially inspired by the works of [37] and [13]. The basic idea is to exploit the local equivalence between the  $\ell_p$  norm [13, Theorem 9] and the weighted  $\ell_1$  norm. Additionally, we leverage measures of optimality for the  $\ell_1$  regularization convex optimization problem as introduced in FARSA [37]. Starting with  $\mathbf{x}^k$  at the  $k$ th iteration, we use the concavity of  $|\cdot|_p^p$  over  $\mathbb{R}_{++}$  to form the following locally weighted  $\ell_1$  regularized minimization model:

$$\min_{\mathbf{x} \in \mathbb{R}^n} G_k(\mathbf{x}) = f(\mathbf{x}) + \sum_{i=1}^n \omega_i^k |x_i|, \quad (11)$$

where  $\omega_i^k = \lambda p(|x_i^k| + \epsilon_i^k)^{p-1}$ ,  $\forall i \in [n]$ . By [1, Theorem 10.1 & Exercise 8.8(c)], similar to Definition 1, we say that an  $\mathbf{x} \in \mathbb{R}^n$  is a first-order stationary point of problem (11) if

$$0 \in \nabla_i f(\mathbf{x}) + \omega_i^k \partial |x_i|, \quad \forall i \in [n]. \quad (12)$$

The following lemma reveals a relationship in terms of the stationarity at a solution estimate between the locally approximated model  $G_k(\mathbf{x})$  and the perturbed  $F(\mathbf{x}; \boldsymbol{\epsilon}^k)$ .

**Lemma 1** *Consider (6) and (11). The following statements are equivalent:*

- (i)  $\mathbf{x}$  is first-order stationary for (11).
- (ii)  $\mathbf{x}$  is first-order stationary for (6) with  $\boldsymbol{\epsilon} = \boldsymbol{\epsilon}^k$ .
- (iii)  $\mathbf{x} = \mathbb{S}_{\boldsymbol{\omega}^k}(\mathbf{x} - \nabla f(\mathbf{x}))$ .

*Proof* The statement holds true by noting that

$$(i) \xrightarrow{(12)} -\nabla f(\mathbf{x}) \in \langle \boldsymbol{\omega}^k, \partial \|\mathbf{x}\|_1 \rangle \iff (\mathbf{x} + \langle \boldsymbol{\omega}^k, \partial \|\mathbf{x}\|_1 \rangle) \ni (\mathbf{x} - \nabla f(\mathbf{x})) \quad (13)$$

$$\iff (iii) \iff (7) \text{ is satisfied} \iff (ii).$$

This completes the proof.

Let  $(\mathbf{x}, \boldsymbol{\epsilon})$  be a solution estimate. For ease of presentation, define the following index sets:

$$\begin{aligned} \kappa_1(\mathbf{x}) &= \{i \in [n] \mid \nabla_i f(\mathbf{x}) + \omega_i < 0\}, \quad \kappa_2(\mathbf{x}) = \{i \in [n] \mid \nabla_i f(\mathbf{x}) - \omega_i > 0\}, \\ \kappa_3(\mathbf{x}) &= \{i \in [n] \mid \nabla_i f(\mathbf{x}) + \omega_i > 0\}, \quad \kappa_4(\mathbf{x}) = \{i \in [n] \mid \nabla_i f(\mathbf{x}) - \omega_i < 0\}. \end{aligned}$$

We also define two stationarity residuals,  $\Psi(\mathbf{x}; \boldsymbol{\epsilon})$  and  $\Phi(\mathbf{x}; \boldsymbol{\epsilon})$ , corresponding to zeros and nonzeros at  $(\mathbf{x}; \boldsymbol{\epsilon})$ , respectively. That is,

$$[\Psi(\mathbf{x}; \boldsymbol{\epsilon})]_i := \begin{cases} \nabla_i f(\mathbf{x}) + \omega_i, & \text{if } i \in \mathcal{I}_0(\mathbf{x}) \cap \kappa_1(\mathbf{x}), \\ \nabla_i f(\mathbf{x}) - \omega_i, & \text{if } i \in \mathcal{I}_0(\mathbf{x}) \cap \kappa_2(\mathbf{x}), \\ 0, & \text{otherwise;} \end{cases} \quad (14)$$

and

$$[\Phi(\mathbf{x}; \boldsymbol{\epsilon})]_i := \begin{cases} 0, & \text{if } i \in \mathcal{I}_0(\mathbf{x}), \\ \min\{\nabla_i f(\mathbf{x}) + \omega_i, \max\{x_i, \nabla_i f(\mathbf{x}) - \omega_i\}\}, & \text{if } i \in \mathcal{I}_+(\mathbf{x}) \cap \kappa_3(\mathbf{x}), \\ \max\{\nabla_i f(\mathbf{x}) - \omega_i, \min\{x_i, \nabla_i f(\mathbf{x}) + \omega_i\}\}, & \text{if } i \in \mathcal{I}_-(\mathbf{x}) \cap \kappa_4(\mathbf{x}), \\ \nabla_i f(\mathbf{x}) + \omega_i \cdot \text{sgn}(x_i), & \text{otherwise.} \end{cases} \quad (15)$$

We provide some intuitive arguments on the defined stationarity residuals.

*Remark 2* Consider that if the stationarity condition (8) holds at  $(\mathbf{x}; \boldsymbol{\epsilon})$ , then  $|\nabla_i f(\mathbf{x})| \leq \omega_i$  for any  $i \in \mathcal{I}_0(\mathbf{x})$ . This indicates that  $|\Psi(\mathbf{x}; \boldsymbol{\epsilon})|$  reflects how close the zero components are to being stationary for (6). For  $i \in \mathcal{I}_+(\mathbf{x}) \cup \mathcal{I}_-(\mathbf{x})$ , the stationarity condition (8) results in  $\nabla_i f(\mathbf{x}) + \omega_i \cdot \text{sgn}(x_i) = 0$ . Thus,  $|\Phi(\mathbf{x}; \boldsymbol{\epsilon})|$  indicates how close the nonzero components are being to stationary for (6). Additionally, the stationarity residual  $[\Phi(\mathbf{x}; \boldsymbol{\epsilon})]_i$  measures the distance that a nonzero component may shift before it becomes zero.

*Remark 3* The defined stationarity residuals for zero and nonzero components motivate the development of a subspace method that minimizes different sets of variables at each iteration. In the proposed algorithm, these residuals serve as the “switching sign” for optimizing zero versus nonzero components. If  $\|\Psi(\mathbf{x}, \boldsymbol{\epsilon})\| \geq \gamma \|\Phi(\mathbf{x}, \boldsymbol{\epsilon})\|$  for some prescribed  $\gamma \in (0, +\infty)$ , it suggests that the zero components

of  $\mathbf{x}$  have a relatively greater impact on the stationarity residual than the nonzero components. Consequently, we perform the minimization in the reduced space  $\mathbb{R}^{|\mathcal{W}|}$  with  $\mathcal{W} \subseteq \{i : [\Psi(\mathbf{x}, \boldsymbol{\epsilon})]_i \neq 0\}$  such that  $\|[\Psi(\mathbf{x}, \boldsymbol{\epsilon})]_{\mathcal{W}}\| \geq \eta_{\Psi} \|\Psi(\mathbf{x}, \boldsymbol{\epsilon})\|$  with  $\eta_{\Psi} \in (0, 1)$ . Conversely, if  $\|\Psi(\mathbf{x}, \boldsymbol{\epsilon})\| < \gamma \|\Phi(\mathbf{x}, \boldsymbol{\epsilon})\|$ , it indicates that the nonzero components of  $\mathbf{x}$  have a relatively greater impact on the stationarity residual than the zero components. In this case, we perform the minimization in the reduced space  $\mathbb{R}^{|\mathcal{W}|}$  with  $\mathcal{W} \subseteq \{i : [\Phi(\mathbf{x}, \boldsymbol{\epsilon})]_i \neq 0\}$  such that  $\|[\Phi(\mathbf{x}, \boldsymbol{\epsilon})]_{\mathcal{W}}\| \geq \eta_{\Phi} \|\Phi(\mathbf{x}, \boldsymbol{\epsilon})\|$  with  $\eta_{\Phi} \in (0, 1)$ . A detailed discussion of this approach is presented in the subsequent sections.

The following lemma provides a formal understanding of stationarity measures (14) and (15).

**Proposition 2** *Consider (14) and (15). The following statements hold.*

(i) *For any  $(\mathbf{x}; \boldsymbol{\epsilon})$  with  $\boldsymbol{\epsilon} \in \mathbb{R}_{++}^n$  and  $\boldsymbol{\omega} = \boldsymbol{\omega}(\mathbf{x}; \boldsymbol{\epsilon})$ , it holds that*

$$|[\Phi(\mathbf{x}; \boldsymbol{\epsilon})]_i| \leq |\nabla_i F(\mathbf{x}; \boldsymbol{\epsilon})|, \quad i \in \mathcal{I}(\mathbf{x}). \quad (16)$$

(ii) *Let  $d(\mu) := \mathbb{S}_{\mu\boldsymbol{\omega}}(\mathbf{x} - \mu \nabla f(\mathbf{x})) - \mathbf{x}$  for  $\mu > 0$ , the following decomposition holds:*

$$d(1) = -[\Psi(\mathbf{x}; \boldsymbol{\epsilon}) + \Phi(\mathbf{x}; \boldsymbol{\epsilon})]. \quad (17)$$

*More generally,*

$$d_i(\mu) = -\mu [\Psi(\mathbf{x}; \boldsymbol{\epsilon})]_i, \quad i \in \mathcal{I}_0(\mathbf{x}), \quad (18a)$$

$$|d_i(\mu)| \geq \min\{\mu, 1\} |[\Phi(\mathbf{x}; \boldsymbol{\epsilon})]_i|, \quad i \in \mathcal{I}(\mathbf{x}). \quad (18b)$$

(iii)  $\mathbf{x}$  satisfies the first-order stationary condition (8) if

$$\|\Phi(\mathbf{x}; \boldsymbol{\epsilon})\| = \|\Psi(\mathbf{x}; \boldsymbol{\epsilon})\| = 0. \quad (19)$$

*Additionally, if  $\epsilon_i = 0$  for  $i \in \mathcal{I}(\mathbf{x})$ , then (19) implies that  $\mathbf{x}$  satisfies the first-order stationary condition (5).*

(iv) *Suppose  $\|\Phi(\mathbf{x}; \boldsymbol{\epsilon})\| \neq 0$  and  $\|\Psi(\mathbf{x}; \boldsymbol{\epsilon})\| \neq 0$ . Then  $\mathcal{W}_{\Phi} \subseteq \{i : [\Phi(\mathbf{x}; \boldsymbol{\epsilon})]_i \neq 0\} \subseteq \mathcal{I}(\mathbf{x})$  or  $\mathcal{W}_{\Psi} \subseteq \{i : [\Psi(\mathbf{x}; \boldsymbol{\epsilon})]_i \neq 0\} \subseteq \mathcal{I}_0(\mathbf{x})$  are nonempty.*

*Proof* (i) We consider the last three cases presented in (15). For  $i \in \mathcal{I}_+(\mathbf{x})$ , we have  $\nabla_i F(\mathbf{x}; \boldsymbol{\epsilon}) = \nabla_i f(\mathbf{x}) + \omega_i$  by (8). When  $i \in \mathcal{I}_+(\mathbf{x}) \cap \kappa_3(\mathbf{x})$ , we also have that  $[\Phi(\mathbf{x}; \boldsymbol{\epsilon})]_i = \min\{\nabla_i f(\mathbf{x}) + \omega_i, x_i\} \leq \nabla_i f(\mathbf{x}) + \omega_i$  if  $\nabla_i f(\mathbf{x}) - \omega_i < 0$ , and otherwise  $[\Phi(\mathbf{x}; \boldsymbol{\epsilon})]_i = \min\{\nabla_i f(\mathbf{x}) + \omega_i, \nabla_i f(\mathbf{x}) - \omega_i\} \leq \nabla_i f(\mathbf{x}) + \omega_i$ . As for the last case, it is obvious that  $[\Phi(\mathbf{x}; \boldsymbol{\epsilon})]_i = \nabla_i f(\mathbf{x}) + \omega_i = \nabla_i F(\mathbf{x}; \boldsymbol{\epsilon})$ . On the other hand, similar arguments can be applied when  $i \in \mathcal{I}_-(\mathbf{x}) \cap \kappa_4(\mathbf{x})$ . Overall, we have shown that (16) holds.

(ii) The proof of (17) can be found in [37, Lemma A.1]. It indicates that  $\Psi(\mathbf{x}; \boldsymbol{\epsilon}) = -d_i(1)$ ,  $i \in \mathcal{I}_0(\mathbf{x})$  and  $\Phi(\mathbf{x}; \boldsymbol{\epsilon}) = -d_i(1)$ ,  $i \in \mathcal{I}(\mathbf{x})$  by the complementarity of  $\Psi$  and  $\Phi$ . This, together with Lemma 7 shown in Appendix, implies (18a) and (18b).

(iii) If (19) is satisfied, then (8) holds by (17) and (13). Moreover, if  $\epsilon_i = 0$ ,  $i \in \mathcal{I}(\mathbf{x})$ , it follows from (9) that  $\mathbf{x}$  satisfies the first-order stationary condition (5).

(iv) Obvious. This completes the proof of all statements.

Proposition 2(iii) implies a practical termination condition for the proposed algorithm. Specifically, when  $\max\{\|\Psi(\mathbf{x}; \boldsymbol{\epsilon})\|, \|\Phi((\mathbf{x}; \boldsymbol{\epsilon}))\|\}$  and  $\epsilon_i, i \in \mathcal{I}(\mathbf{x})$  are relatively small, the solution estimate  $\mathbf{x}$  is nearly a stationary point of  $(\mathcal{P})$ . This proposition also informs the updating strategy for  $\boldsymbol{\epsilon} \in \mathbb{R}_{++}^n$ . A reasonable updating strategy should rapidly drive  $\epsilon_i, i \in [n]$  associated with the nonzeros of  $\mathbf{x}$ , to zero once the correct support  $\mathcal{I}(\mathbf{x})$  is identified. Meanwhile,  $\epsilon_i, i \in \mathcal{I}_0(\mathbf{x})$  should be fixed as constants [13]. The key idea behind this strategy is to eliminate the zeros and the associated  $\epsilon_i$  from  $F(\mathbf{x}; \boldsymbol{\epsilon})$ , thereby transforming the problem into a smooth one. This transformation is crucial for the convergence analysis. In SOIR $\ell_1$ , we only decrease  $\epsilon_i, i \in [n]$  associated with the nonzeros of  $\mathbf{x}$  (lines 6 and 25 of Algorithm 1).

### 3.2 Reduced-space Proximal Weighted $\ell_1$ Regularized Subproblem

The sequence generated by SOIR $\ell_1$  consists of solution estimates obtained either by solving subspace proximal first-order approximate subproblems or by solving subspace regularized Newton subproblems. To correctly identify the support of a desired stationary point and ensure global convergence, we construct an approximate model of (11) by replacing the function  $f$  with its locally linear approximation and a proximal term while retaining the weighted  $\ell_1$ -norm restricted to a subset of the nonzero variables (refer to lines 11 and 14 of Algorithm 1), i.e.,

$$\min_{\mathbf{x}_{\mathcal{W}} \in \mathbb{R}^{|\mathcal{W}|}} Q_{\mu_k}(\mathbf{x}_{\mathcal{W}}; \mathbf{x}^k) = \langle \nabla_{\mathcal{W}} f(\mathbf{x}^k), \mathbf{x}_{\mathcal{W}} - \mathbf{x}_{\mathcal{W}}^k \rangle + \frac{1}{2\mu_k} \|\mathbf{x}_{\mathcal{W}} - \mathbf{x}_{\mathcal{W}}^k\|_2^2 + \sum_{i \in \mathcal{W}} \omega_i^k |x_i| \quad (20)$$

where  $\mathcal{W} \subset [n]$  is formed according to the relative impact of zeros and nonzeros of the current iterate and  $\mu_k > 0$ . The formed subproblem highlights a notable difference between SOIR $\ell_1$  and HpgSRN [36]. Subproblem (20) admits a closed-form solution  $\mathbf{x}_{\mathcal{W}}^* = [\mathbb{S}_{\mu\omega^k}(\mathbf{x}^k - \mu_k \nabla f(\mathbf{x}^k))]_{\mathcal{W}}$  in a low-dimensional space  $\mathbb{R}^{|\mathcal{W}|}$ , which can be computed efficiently. In contrast, HpgSRN requires a proximal gradient method to solve the subproblem in the full  $n$ -dimensional space iteratively. To ensure global convergence, we use a simple variant of the inexact line-search with backtracking to find a proper value of  $\mu_k$  such that  $G_k(\mathbf{x}^j) < G_k(\mathbf{x}) - \frac{\alpha}{2} \|\mathbf{x}^j - \mathbf{x}\|^2$  is satisfied, where  $\mathbf{x}^j$  a solution estimate in the  $j$ th iteration of Algorithm 2 and  $\alpha > 0$  is a prescribed scalar.

---

**Algorithm 2** IST step:  $[\mathbf{x}^j, \mu_j] := \text{IST}(\mathbf{x}, \boldsymbol{\omega}, \mathcal{W}; \alpha, \xi, \bar{\mu})$ 


---

**Require:**  $\{\mathbf{x}, \boldsymbol{\omega}\} \in \mathbb{R}^n$ ,  $\mathcal{W} \subseteq [n]$ ;  $\{\bar{\mu}, \alpha\} \in (0, +\infty)$  and  $\xi \in (0, 1)$ .

- 1: Let  $\mu_0 \leftarrow \bar{\mu}$  and  $\mathbf{x}_{\mathcal{W}^c}^0 \leftarrow \mathbf{x}_{\mathcal{W}^c}$ ,  $\mathbf{x}_{\mathcal{W}}^0 \leftarrow [\mathbb{S}_{\mu_0 \boldsymbol{\omega}}(\mathbf{x} - \mu_0 \nabla f(\mathbf{x}))]_{\mathcal{W}}$ .
- 2: **for**  $j = 0, 1, 2, \dots$  **do**
- 3:   **if**  $G_k(\mathbf{x}^j) \leq G_k(\mathbf{x}) - \frac{\alpha}{2} \|\mathbf{x}^j - \mathbf{x}\|^2$  **then**
- 4:     **return**  $\mathbf{x}^j$ .
- 5:   **end if**
- 6:    $\mu_{j+1} \leftarrow \xi \mu_j$ .
- 7:    $\mathbf{x}_{\mathcal{W}^c}^{j+1} \leftarrow \mathbf{x}_{\mathcal{W}^c}$ ,  $\mathbf{x}_{\mathcal{W}}^{j+1} \leftarrow [\mathbb{S}_{\mu_{j+1} \boldsymbol{\omega}}(\mathbf{x} - \mu_{j+1} \nabla f(\mathbf{x}))]_{\mathcal{W}}$ .
- 8: **end for**

---

For ease of presentation, we drop the iteration counter superscript  $k$  in the outer loop in Algorithm 2. The following lemma proves that the line-search with backtracking, as described in lines 2–8 of Algorithm 2, terminates in a finite number of steps.

**Lemma 2** *Suppose Algorithm 2 is executed by calling  $(\hat{\mathbf{x}}, \hat{\mu}) = IST(\mathbf{x}, \boldsymbol{\omega}, \mathcal{W}; \alpha, \xi, \bar{\mu})$ . Then, Algorithm 2 determines in a finite number of iterations a value  $\hat{\mu}$  that satisfies the condition from line 3 of Algorithm 2. Moreover, it holds that*

$$\min\{\bar{\mu}, \frac{\xi}{L_1(\mathbf{x}) + \alpha}\} \leq \hat{\mu} \leq \bar{\mu} \quad (21)$$

with  $L_1(\mathbf{x}) > 0$  and

$$F(\hat{\mathbf{x}}, \boldsymbol{\epsilon}) - F(\mathbf{x}, \boldsymbol{\epsilon}) \leq G(\hat{\mathbf{x}}) - G(\mathbf{x}) \leq -\frac{\alpha}{2} \|\hat{\mathbf{x}} - \mathbf{x}\|^2. \quad (22)$$

*Proof* We first provide some local properties on the function  $\nabla f$  restricted to a reduced space. For each  $j \in \mathbb{N}$ , we have from  $\mu_j \leq \bar{\mu}$  (see line 6) and  $\mathbf{x}_{\mathcal{W}}^j = [\mathbb{S}_{\mu_j} \boldsymbol{\omega}(\mathbf{x} - \mu_j \nabla f(\mathbf{x})]_{\mathcal{W}}$  and  $\mathbf{x}_{\mathcal{W}^c}^j = \mathbf{x}_{\mathcal{W}^c}$  that

$$\begin{aligned} Q_{\bar{\mu}}(\mathbf{x}_{\mathcal{W}}^j; \mathbf{x}) &\leq \langle \nabla_{\mathcal{W}} f(\mathbf{x}), \mathbf{x}_{\mathcal{W}}^j - \mathbf{x}_{\mathcal{W}} \rangle + \frac{1}{2\mu_j} \|\mathbf{x}_{\mathcal{W}} - \mathbf{x}_{\mathcal{W}}^j\|_2^2 + \sum_{i \in \mathcal{W}} \boldsymbol{\omega}_i |\mathbf{x}_i^j| \\ &\leq \sum_{i \in \mathcal{W}} \boldsymbol{\omega}_i |\mathbf{x}_i| = Q_{\bar{\mu}}(\mathbf{x}_{\mathcal{W}}; \mathbf{x}). \end{aligned} \quad (23)$$

Since  $Q_{\bar{\mu}}(\cdot; \mathbf{x})$  is continuous and coercive, we know that the level set  $\text{Lev}_{Q_{\bar{\mu}}(\cdot; \mathbf{x})} := \{\mathbf{z} \in \mathbb{R}^{|\mathcal{W}|} : Q_{\bar{\mu}}(\mathbf{z}; \mathbf{x}) \leq Q_{\bar{\mu}}(\mathbf{x}_{\mathcal{W}}; \mathbf{x})\}$  is compact. Additionally, since  $\nabla_{\mathcal{W}} f$  is continuously differentiable, we know that there exists  $L_1(x)$  such that for any  $\mathbf{y}, \mathbf{z} \in \text{Lev}_{Q_{\bar{\mu}}(\cdot; \mathbf{x})}$ ,

$$\|\nabla_{\mathcal{W}} f(\mathbf{y}) - \nabla_{\mathcal{W}} f(\mathbf{z})\| \leq L_1(x) \|\mathbf{y} - \mathbf{z}\|. \quad (24)$$

We now prove the statement by seeking a contradiction. Suppose Algorithm 2 with backtracking cycles indefinitely between line 3 and 7. Then line 3 of Algorithm 2 is never implemented, and hence for any trial point  $\mathbf{x}^j$  with  $j \in \mathbb{N}$ , it holds that

$$G(\mathbf{x}^j) > G(\mathbf{x}) - \frac{\alpha}{2} \|\mathbf{x}^j - \mathbf{x}\|^2. \quad (25)$$

Note however that  $\xi \in (0, 1)$  and  $\mu_j \rightarrow 0$  as  $j \rightarrow +\infty$  and therefore, for  $j \rightarrow +\infty$   $\mathbf{x}_{\mathcal{W}}^j = [\mathbb{S}_{\mu_j} \boldsymbol{\omega}(\mathbf{x} - \mu_j \nabla f(\mathbf{x})]_{\mathcal{W}} \rightarrow \mathbf{x}_{\mathcal{W}}$  since  $\nabla_{\mathcal{W}} f(\mathbf{x})$  is bounded over  $\text{Lev}_{Q_{\bar{\mu}}(\cdot; \mathbf{x})}$ . This, together with the continuity of  $G(\cdot)$  and  $\|\cdot\|^2$ , gives  $\lim_{j \rightarrow +\infty} G(\mathbf{x}^j) = G(\mathbf{x})$  and  $\|\mathbf{x}^j - \mathbf{x}\|^2 \rightarrow 0$ . By (25), the contradiction  $0 > 0$  shows that the exists a finite  $j_0$  such that  $G(\mathbf{x}^{j_0}) \leq G(\mathbf{x}) - \frac{\alpha}{2} \|\mathbf{x}^j - \mathbf{x}\|^2$ .

Recall that  $\mathbf{x}_{\mathcal{W}}^j = [\mathbb{S}_{\mu_j} \boldsymbol{\omega}(\mathbf{x} - \mu_j \nabla f(\mathbf{x})]_{\mathcal{W}}$  and  $\mathbf{x}_{\mathcal{W}^c}^j = \mathbf{x}_{\mathcal{W}^c}$ , then we have

$$\langle \nabla f(\mathbf{x}), \mathbf{x}^j - \mathbf{x} \rangle + \frac{1}{2\mu_j} \|\mathbf{x}^j - \mathbf{x}\|^2 + \sum_{i=1}^n \omega_i |\mathbf{x}_i^j| \leq \sum_{i=1}^n \omega_i |\mathbf{x}_i|. \quad (26)$$

It follows from (24) and (26) that for any  $\mu_j \leq \frac{1}{L_1(\mathbf{x})+\alpha}$ ,

$$\begin{aligned}
G(\mathbf{x}^j) &\leq f(\mathbf{x}) + \langle \nabla f(\mathbf{x}), \mathbf{x}^j - \mathbf{x} \rangle + \frac{L_1(\mathbf{x})}{2} \|\mathbf{x}^j - \mathbf{x}\|^2 + \sum_{i=1}^n \omega_i |\mathbf{x}_i^j| \\
&\leq f(\mathbf{x}) + \langle \nabla f(\mathbf{x}), \mathbf{x}^j - \mathbf{x} \rangle + \frac{1}{2\mu_j} \|\mathbf{x}^j - \mathbf{x}\|^2 + \sum_{i=1}^n \omega_i |\mathbf{x}_i^j| - \frac{\alpha}{2} \|\mathbf{x}^j - \mathbf{x}\|^2 \\
&\leq f(\mathbf{x}) + \sum_{i=1}^n \omega_i |\mathbf{x}_i| - \frac{\alpha}{2} \|\mathbf{x}^j - \mathbf{x}\|^2 \\
&= G(\mathbf{x}) - \frac{\alpha}{2} \|\mathbf{x}^j - \mathbf{x}\|^2
\end{aligned} \tag{27}$$

Therefore, we have  $\min\{\bar{\mu}, \frac{\xi}{L_1(\mathbf{x})+\alpha}\} \leq \mu_{j_0} \leq \bar{\mu}$ . Denote  $\hat{\mathbf{x}} = \mathbf{x}^{j_0}$ . We have from the concavity of  $|\cdot|^p$  over  $\mathbb{R}_{++}$  that

$$\lambda [(|\hat{x}_i| + \epsilon_i)^p - (|x_i| + \epsilon_i)^p] \leq \omega_i (|\hat{x}_i| - |x_i|). \tag{28}$$

It then follows from (22) and (28) that (22) holds. This completes the proof.

We show some useful properties in the following lemma.

**Lemma 3** *Consider Algorithm 1. Suppose the termination criterion of Algorithm 1 is not satisfied. Then the following hold.*

(i) *If  $\|\Psi(\mathbf{x}^k; \boldsymbol{\epsilon}^k)\| \geq \gamma \|\Phi(\mathbf{x}^k; \boldsymbol{\epsilon}^k)\|$  and lines 10 and 11 are executed. Then  $\mathcal{I}^k \subseteq \mathcal{I}^{k+1}$ . Indeed, it holds that*

$$\mathcal{I}^{k+1} = \mathcal{I}^k \cup \mathcal{W}_k \text{ and } |\mathcal{I}^{k+1}| = |\mathcal{I}^k| + |\mathcal{W}_k|. \tag{29}$$

(ii) *If  $\|\Psi(\mathbf{x}^k; \boldsymbol{\epsilon}^k)\| < \gamma \|\Phi(\mathbf{x}^k; \boldsymbol{\epsilon}^k)\|$  and lines 13 and 14 are executed, but line 15 is not triggered. Then  $\mathcal{I}^k \supset \mathcal{I}^{k+1}$ .*

*Proof* (i). Suppose  $\|\Psi(\mathbf{x}^k; \boldsymbol{\epsilon}^k)\| \geq \gamma \|\Phi(\mathbf{x}^k; \boldsymbol{\epsilon}^k)\|$ . Then

$$\emptyset \neq \mathcal{W}_k \subseteq \{i : [\Psi(\mathbf{x}^k; \boldsymbol{\epsilon}^k)]_i \neq 0\} \subseteq \mathcal{I}_0^k \tag{30}$$

is chosen (see line 10 of Algorithm 1) such that the norm of  $\Psi(\mathbf{x}^k; \boldsymbol{\epsilon}^k)$  over  $\mathcal{W}_k$  is greater than a fraction of  $\Psi(\mathbf{x}^k; \boldsymbol{\epsilon}^k)$  over all components, and SOIR $\ell_1$  calls the subroutine IST step (see line 11) in the reduced space  $\mathbb{R}^{|\mathcal{W}_k|}$  and gives a solution estimate  $\mathbf{x}^{k+1}$ . We therefore conclude that  $\mathcal{I}^k \subseteq \mathcal{I}^{k+1}$ , meaning zero components could become nonzero in this step. In fact, by Proposition 2(ii) and (30), we have

$$x_i^{k+1} - x_i^k = \mu_k [\Psi(\mathbf{x}^k; \boldsymbol{\epsilon}^k)]_i \neq 0, i \in \mathcal{W}_k.$$

Then, we know  $\mathcal{I}^{k+1} = \mathcal{I}^k \cup \mathcal{W}_k$  and  $\mathcal{I}^k \cap \mathcal{W}_k = \emptyset$ . Hence,  $|\mathcal{I}^{k+1}| = |\mathcal{I}^k| + |\mathcal{W}_k|$ .

(ii). Suppose  $\|\Psi(\mathbf{x}^k; \boldsymbol{\epsilon}^k)\| < \gamma \|\Phi(\mathbf{x}^k; \boldsymbol{\epsilon}^k)\|$ . Then

$$\emptyset \neq \mathcal{W}_k \subseteq \{i : \Phi_i^k \neq 0\} \subseteq \mathcal{I}^k \tag{31}$$

is chosen (see line 13) such that the norm of  $\Phi^k$  over this subset is greater than a fraction of  $\Phi^k$  over all components, SOIR $\ell_1$  calls the subroutine IST step (see line 14) in the reduced space  $\mathbb{R}^{|\mathcal{W}_k|}$  and gives a solution estimate  $\hat{\mathbf{x}}^{k+1}$ . If  $\text{sgn}(\hat{\mathbf{x}}^{k+1}) \neq \text{sgn}(\mathbf{x}^k)$  (see line 15), then  $\hat{\mathbf{x}}^{k+1}$  is accepted as the next iterate (see line 22). We then conclude that  $\mathcal{I}^k \supset \mathcal{I}^{k+1}$ , meaning zero components could become nonzeros in this step. This completes the proof.

### 3.3 Reduced-space Quadratic Subproblems

In [13, Theorem 4], the authors demonstrated that the  $\text{IR}\ell_1$  algorithm exhibits a locally stable sign property. Specifically, the sign of the sequence generated by  $\text{IR}\ell_1$  remains fixed after a certain number of iterations. The locally stable sign property naturally follows from the stable support property [13, Theorem 3]. Once the support is identified, a more efficient second-order method can be applied to the nonzero elements in the support to accelerate the local convergence rate. While these properties are advantageous, it is generally not possible to know in advance whether the support has been identified. To overcome this challenge, at the  $k$ th iteration  $\mathbf{x}^k$ , when it is observed that two successive iterates,  $\mathbf{x}^k$  and  $\hat{\mathbf{x}}^{k+1}$  return by IST step, share the same sign (see line 15),  $\text{SOIR}\ell_1$  minimizes a quadratic subproblem restricted to a subset of nonzero variables (lines 16–19), which reads

$$\min_{\mathbf{d} \in \mathbb{R}^{|\mathcal{W}_k|}} m_k(\mathbf{d}) := \langle \mathbf{g}^k, \mathbf{d} \rangle + \frac{1}{2} \langle \mathbf{d}, \mathbf{H}^k \mathbf{d} \rangle, \quad (32)$$

where  $\mathbf{g}^k = \nabla_{\mathcal{W}_k} F(\mathbf{x}^k; \boldsymbol{\epsilon}^k)$  is the subspace gradient of  $F(\mathbf{x}^k; \boldsymbol{\epsilon}^k)$  and  $\mathbf{H}^k = \nabla_{\mathcal{W}_k \mathcal{W}_k}^2 F(\mathbf{x}^k; \boldsymbol{\epsilon}^k) + \zeta \mathbf{I} \succ \mathbf{0}$  is a modified subspace Hessian matrix related to  $F(\mathbf{x}^k; \boldsymbol{\epsilon}^k)$  with  $\zeta_k \in (0, +\infty)$ . Since the working index set  $\mathcal{W}_k \subseteq \mathcal{I}(\mathbf{x}^k)$  is nonempty by Proposition 2, the objective function  $F(\mathbf{x}; \boldsymbol{\epsilon})$  is smooth with respect to the variables restricted to  $\mathcal{W}_k$  at  $\mathbf{x}^k$ .

Since the local quadratic model  $m_k$  is constructed in the reduced space  $\mathbb{R}^{|\mathcal{W}_k|}$ , it often has a relatively small dimension. Consequently, problem (32) can be efficiently solved by many existing quadratic programming methods, such as the Conjugate Gradient (CG) method. It is worth noting that  $\text{SOIR}\ell_1$  is independent of the choice of the subproblem solver.

When the correct support of an optimal solution is detected, an exact subspace Hessian of the objective function  $F$  is employed in the neighborhood of the optimization point, causing the algorithm to revert to a classic Newton method. Otherwise, the unboundedness of  $\mathbf{H}^k$  should be addressed. One simple technique is given by the Levenberg-Marquardt method, which modifies the Hessian by adding a multiple of identity matrix to ensure positive definiteness and hence yield a descent search direction. Another technique is to consider a trust region for the search direction to avoid unboundedness, typically requiring a tailored solver to find the (global) optimal solution of the subproblem. This discussion will be deferred to a later section.

It should be noted that an exact minimizer of  $m_k$  is not required to be found by the subproblem solver during each iteration. Let  $\mathbf{d}_R^k$  be a reference direction, computed by minimizing  $m_k$  along the steepest descent direction (see line 17). We permit an inexact solution estimate of (32) as long as the solution  $\bar{\mathbf{d}}^k$  results in a reduction of the objective  $m_k$  and, is more effective than  $\mathbf{d}_R^k$  (see line 18). Specifically,  $m_k(\bar{\mathbf{d}}^k) \leq m_k(\mathbf{0})$  and  $\langle \mathbf{g}^k, \bar{\mathbf{d}}^k \rangle \leq \langle \mathbf{g}^k, \mathbf{d}_R^k \rangle$ . We use  $\bar{\mathbf{d}}^k$  to update the variables in  $\mathcal{W}_k$ , setting the search direction  $\mathbf{d}^k \in \mathbb{R}^n$  accordingly (see line 19). Therefore, after obtaining an inexact solution of the reduced QP subproblem (32), we achieve the following result.

**Lemma 4** *Consider the reduced-space QP subproblem (32) with  $\mathbf{H}^k \succ \mathbf{0}$  being obtained from line 16 of Algorithm 1. Then  $\mathbf{H}^k$  is bounded and uniformly positive*

definite, i.e., there exist  $0 < \bar{\lambda}_{\min} < \bar{\lambda}_{\max} < +\infty$  such that

$$\bar{\lambda}_{\min} \|\mathbf{z}\|^2 \leq \langle \mathbf{z}, \mathbf{H}^k \mathbf{z} \rangle \leq \bar{\lambda}_{\max} \|\mathbf{z}\|^2, \quad \forall \mathbf{z} \in \mathbb{R}^{|\mathcal{W}_k|}. \quad (33)$$

Moreover, the following inequalities hold.

$$\langle \mathbf{g}^k, \bar{\mathbf{d}}^k \rangle \leq \langle \mathbf{g}^k, \mathbf{d}_R^k \rangle < 0, \quad (34)$$

$$|\langle \mathbf{g}^k, \bar{\mathbf{d}}^k \rangle| \geq |\langle \mathbf{g}^k, \mathbf{d}_R^k \rangle| = \frac{\|\mathbf{g}^k\|^2}{\langle \mathbf{g}^k, \mathbf{H}^k \mathbf{g}^k \rangle} \|\mathbf{g}^k\|^2 \geq \frac{\|\mathbf{g}^k\|^2}{\bar{\lambda}_{\max}}, \quad (35)$$

$$\frac{\|\mathbf{g}^k\|}{\bar{\lambda}_{\max}} \leq \|\bar{\mathbf{d}}^k\| \leq \frac{2\|\mathbf{g}^k\|}{\bar{\lambda}_{\min}}. \quad (36)$$

*Proof* By Assumption 1(i), we know that the level set  $\text{Lev}_F := \{\mathbf{x} \in \mathbb{R}^n : F(\mathbf{x}, \boldsymbol{\epsilon}) \leq F(\mathbf{x}^0, \boldsymbol{\epsilon}^0)\}$  is compact by noting that  $F$  is continuous and coercive. It follows the compactness of  $\text{Lev}_F$  that  $f$  is Lipschitz differentiable on  $\text{Lev}_F$  with Lipschitz constant  $L_f > 0$ , and there exists a constant  $\tilde{L}_f > 0$  such that  $\|\nabla^2 f(\mathbf{x})\| \leq \tilde{L}_f$  for  $\mathbf{x} \in \text{Lev}_F$ .

Since  $\mathbf{x}^k \in \text{Lev}_F$  and  $\mathbf{H}^k = \nabla_{\mathcal{W}_k}^2 F(\mathbf{x}^k; \boldsymbol{\epsilon}^k) + \zeta \mathbf{I} = \nabla_{\mathcal{W}_k}^2 f(\mathbf{x}) + \lambda p(p-1)\text{diag}([(x + \boldsymbol{\epsilon}^k)_{\mathcal{W}_k}]^{p-2}) + \zeta_k \mathbf{I}$ , we conclude that  $\bar{\lambda}_{\min} \mathbf{I} \preceq \mathbf{H}^k \preceq \bar{\lambda}_{\max} \mathbf{I}$  for some  $0 < \bar{\lambda}_{\min} < \bar{\lambda}_{\max} < +\infty$  due to  $\mathcal{W}_k \subseteq \mathcal{I}(\mathbf{x}^k)$  and  $\zeta_k \in (0, +\infty)$ .

Inequalities (34) and (35) can be easily verified. We hence only prove (36). Let  $\mathbf{d}_N^k$  denote the exact solution (32). It follows from the optimality condition of (32) that

$$\|\mathbf{d}_N^k\| \leq \|(\mathbf{H}^k)^{-1}\| \|\mathbf{g}^k\| \leq \frac{\|\mathbf{g}^k\|}{\bar{\lambda}_{\min}}. \quad (37)$$

Define a quadratic function  $\bar{m}_k(\mathbf{d}) := m_k(\mathbf{d}_N^k + \mathbf{d})$  and the associated level set  $\text{Lev}_{\bar{m}_k} := \{\mathbf{d} : \bar{m}_k(\mathbf{d}) \leq 0\}$ . We then see that

$$(\bar{\mathbf{d}}^k - \mathbf{d}_N^k) \in \text{Lev}_{\bar{m}_k}, \quad (38)$$

since  $\bar{m}_k(\bar{\mathbf{d}}^k - \mathbf{d}_N^k) = m_k(\bar{\mathbf{d}}^k) \leq m_k(\mathbf{0}) = 0$  due to the imposed conditions (10) (see line 18 of Algorithm 1). We have for any  $\mathbf{d} \in \text{Lev}_{\bar{m}_k}$  that

$$\bar{\lambda}_{\min} \|\mathbf{d}\|^2 \leq \langle \mathbf{d}, \mathbf{H}^k \mathbf{d} \rangle \leq -\langle \mathbf{g}^k, \mathbf{d}_N^k \rangle,$$

where the second inequality is from the definition of  $\text{Lev}_{\bar{m}_k}$ . Therefore, we have

$$\|\mathbf{d}\|^2 \leq \frac{-\langle \mathbf{g}^k, \mathbf{d}_N^k \rangle}{\bar{\lambda}_{\min}}.$$

This, together with (37), (38) and the definition of  $\mathbf{d}_N^k$  gives

$$\|\bar{\mathbf{d}}^k - \mathbf{d}_N^k\|^2 \leq \frac{-\langle \mathbf{g}^k, \mathbf{d}_N^k \rangle}{\bar{\lambda}_{\min}} \leq \frac{\|(\mathbf{H}^k)^{-1}\| \|\mathbf{g}^k\|^2}{\bar{\lambda}_{\min}} = \frac{\|\mathbf{g}^k\|^2}{(\bar{\lambda}_{\min})^2}. \quad (39)$$

Combining (39) with the triangle inequality and (37), we obtain

$$\|\bar{\mathbf{d}}^k\| \leq \|\bar{\mathbf{d}}^k - \mathbf{d}_N^k\| + \|\mathbf{d}_N^k\| \leq \frac{\|\mathbf{g}^k\|}{\bar{\lambda}_{\min}} + \frac{\|\mathbf{g}^k\|}{\bar{\lambda}_{\min}} = \frac{2\|\mathbf{g}^k\|}{\bar{\lambda}_{\min}}.$$

In addition,  $\|\bar{\mathbf{d}}^k\| \geq \frac{\|\mathbf{g}^k\|}{\bar{\lambda}_{\max}}$  is straightforward from (35). This completes the proof.

### 3.4 Projected Line-search (Algorithm 3)

Once a descent direction  $\mathbf{d}$  is obtained by inexactly solving (32), SOIR $\ell_1$  implements a projected line-search [37] to determine a stepsize that ensures a sufficient decrease in  $F(\mathbf{x}; \epsilon)$ , as presented in Algorithm 3. We shall interpret Algorithm 3 line-by-line, omitting the iteration counter superscript  $k$  used in Algorithm 1.

Algorithm 3 consists of three main blocks. The first block corresponds to lines 1–8. Starting with  $\mathbf{y}^j$  at the  $j$ th iteration. If  $\text{sgn}(\mathbf{y}^j) \neq \text{sgn}(\mathbf{x})$  holds, a line-search with backtracking is performed along direction  $\mathbf{d}$  to determine a stepsize  $\mu_j$  such that the projection  $\mathbb{P}(\mathbf{x} + \mu_j \mathbf{d}; \mathbf{x})$  causes a decrease in  $F(\mathbf{x}; \epsilon)$ . If such a stepsize is found (i.e., line 3 holds), it is deemed a “successful” step with no deterioration in the objective value and reduced support size. The line-search then terminates with  $\mathbf{y}^j \leftarrow \mathbb{P}(\mathbf{x} + \mu_j \mathbf{d}; \mathbf{x})$ . Otherwise,  $\mathbb{P}(\mathbf{x} + \mu_j \mathbf{d}; \mathbf{x})$  should have the same sign with  $\mathbf{x}$  after finite line-search trials. In this case, the first block terminates with  $j > 0$  and proceeds to the second block (see lines 9–15).

Failure of the line-search with backtracking in the first block indicates that finding an iterate with an improved objective value and reduced support size compared to  $\mathbf{x}^k$  is unlikely. The algorithm then verifies a stepsize  $\mu_B = \arg \sup \{\mu > 0 : \text{sgn}(\mathbf{x} + \mu \mathbf{d}) = \text{sgn}(\mathbf{x})\}$ , which aims to yield a new iterate with reduced support (lines 10). If  $\mathbf{x} + \mu_B \mathbf{d}$  causes a sufficient decrease in  $F(\mathbf{x}; \epsilon)$ , it is also deemed a “successful” stepsize (line 14).

The definition of  $\mu_B$  implies that  $\mu_B$  is no less than the  $\mu_j$  found in the first block. Therefore, if  $\mu_B$  is successful, the algorithm will not proceed to the third block (lines 16–22). If not, the loop in the third block continues the line-search with backtracking, terminating in a finite number of iterations.

Overall, we can conclude that  $\mathcal{I}(\mathbf{y}^j) = \mathcal{I}(\mathbf{x})$  if the Algorithm 3 is terminated in line 18 and  $\mathcal{I}(\mathbf{y}^j) \subset \mathcal{I}(\mathbf{x})$  otherwise. The following lemma summarizes these interpretations of Algorithm 3.

**Lemma 5** *Consider Algorithm 3. Let  $\mathbf{x}, \mathbf{d} \in \mathbb{R}^n$ ,  $\epsilon \in \mathbb{R}_+^n$  and  $\mathcal{W} \subseteq \mathcal{I}(\mathbf{x})$  such that  $\langle \nabla_{\mathcal{W}} F(\mathbf{x}; \epsilon), \mathbf{d}_{\mathcal{W}} \rangle < 0$  and  $\mathbf{d}_{\mathcal{W}^c} = \mathbf{0}$ . Then Algorithm 3 terminates finitely at some iteration number  $j_0$  and generates a value  $\mu_{j_0}$ . Moreover, if  $\text{sgn}(\mathbf{y}^{j_0}) \neq \text{sgn}(\mathbf{x})$ , we have*

$$\mu_{j_0} \geq \min(1, \mu_B) \quad \text{and} \quad |\mathcal{I}(\mathbf{y}^{j_0})| < |\mathcal{I}(\mathbf{x})|. \quad (40)$$

Otherwise,

$$\mu_{j_0} \geq \frac{2\xi(\varpi - 1) \langle \nabla_{\mathcal{W}} F(\mathbf{x}; \epsilon), \mathbf{d}_{\mathcal{W}} \rangle}{L_2(\mathbf{x}) \|\mathbf{d}_{\mathcal{W}}\|^2} \quad \text{and} \quad |\mathcal{I}(\mathbf{y}^{j_0})| = |\mathcal{I}(\mathbf{x})|, \quad (41)$$

where  $L_2(\mathbf{x})$  is the Lipschitz constant of  $F(\mathbf{x}; \epsilon)$  in the neighborhood  $\mathcal{B}(\mathbf{x}, \xi \mu_B \|\mathbf{d}\|)$  of  $\mathbf{x}$  in the subspace  $\mathbb{R}^{\mathcal{W}}$  with  $\xi \in (0, 1)$ .

*Proof* It suffices to restrict the discussion in the reduced space  $\mathbb{R}^{|\mathcal{W}|}$  since  $\mathbf{d}_{\mathcal{W}^c} = \mathbf{0}$ . Since  $\mathbf{x}_{\mathcal{W}}, \mathcal{W} \subseteq \mathcal{I}(\mathbf{x})$  is strictly in the interior of the “subspace orthant”  $\{\mathbf{z}_{\mathcal{W}} \in \mathbb{R}^{|\mathcal{W}|} \mid \text{sgn}(\mathbf{z}_{\mathcal{W}}) = \text{sgn}(\mathbf{x}_{\mathcal{W}})\} \neq \emptyset$  and  $F(\mathbf{x}; \epsilon)$  is smooth in the subspace orthant around  $\mathbf{x}_{\mathcal{W}}$ . Hence, we can remove the subscript  $\mathcal{W}$  for brevity.

If  $\text{sgn}(\mathbf{y}^{j_0}) \neq \text{sgn}(\mathbf{x})$ , then Algorithm 3 terminates by line 4 or line 13. Therefore,  $F(\mathbf{y}^{j_0}; \epsilon) \leq F(\mathbf{x}; \epsilon)$  naturally holds and  $\mathbf{y}^{j_0}$  is on the boundary of subspace orthant containing  $\mathbf{x}$  by (3), meaning  $|\mathcal{I}(\mathbf{y}^{j_0})| < |\mathcal{I}(\mathbf{x})|$ .

If  $\text{sgn}(\mathbf{y}^{j_0}) = \text{sgn}(\mathbf{x})$ , then Algorithm 3 executes line 16–22 and terminates by line 18. When line 16 is reached, there are two cases to consider.

**Algorithm 3** Projected line-search:  $[\mathbf{y}^j, \mu_j] := \text{PLS}(\mathbf{x}; \boldsymbol{\epsilon}, \mathbf{d}, \mathcal{W}; \varpi, \xi)$ 


---

**Require:**  $\{\mathbf{x}, \mathbf{d}, \boldsymbol{\epsilon}\} \in \mathbb{R}^n$ ,  $\mathcal{W} \subseteq \mathcal{I}(\mathbf{x})$ ;  $\varpi \in (0, \frac{1}{2})$  and  $\xi \in (0, 1)$ .

- 1: Set  $j \leftarrow 0$ ,  $\mu_0 \leftarrow 1$  and  $\mathbf{y}^0 \leftarrow \mathbb{P}(\mathbf{x} + \mathbf{d}; \mathbf{x})$ .
- 2: **while**  $\text{sgn}(\mathbf{y}^j) \neq \text{sgn}(\mathbf{x})$  **do**
- 3:   **if**  $F(\mathbf{y}^j; \boldsymbol{\epsilon}) \leq F(\mathbf{x}; \boldsymbol{\epsilon})$  **then**
- 4:     **return**  $\mathbf{y}^j$ .
- 5:   **end if**
- 6:   Set  $j \leftarrow j + 1$  and  $\mu_j = \xi \mu_{j-1}$ .
- 7:   Set  $\mathbf{y}^j \leftarrow \mathbb{P}(\mathbf{x} + \mu_j \mathbf{d}; \mathbf{x})$ .
- 8: **end while**
- 9: **if**  $j \neq 0$  **then**
- 10:   Set  $\mu_B \leftarrow \arg \sup \{\mu > 0 : \text{sgn}(\mathbf{x} + \mu \mathbf{d}) = \text{sgn}(\mathbf{x})\}$ .
- 11:   Set  $\mathbf{y}^j \leftarrow \mathbf{x} + \mu_B \mathbf{d}$ .
- 12:   **if**  $F(\mathbf{y}^j; \boldsymbol{\epsilon}) \leq F(\mathbf{x}; \boldsymbol{\epsilon}) + \varpi \mu_B \langle \nabla_{\mathcal{W}} F(\mathbf{x}; \boldsymbol{\epsilon}), \mathbf{d}_{\mathcal{W}} \rangle$  **then**
- 13:     **return**  $\mathbf{y}^j$ .
- 14:   **end if**
- 15: **end if**
- 16: **loop**
- 17:   **if**  $F(\mathbf{y}^j; \boldsymbol{\epsilon}) \leq F(\mathbf{x}; \boldsymbol{\epsilon}) + \varpi \mu_j \langle \nabla_{\mathcal{W}} F(\mathbf{x}; \boldsymbol{\epsilon}), \mathbf{d}_{\mathcal{W}} \rangle$  **then**
- 18:     **return**  $\mathbf{y}^j$ .
- 19:   **end if**
- 20:   Set  $j \leftarrow j + 1$  and  $\mu_j = \xi \mu_{j-1}$ .
- 21:   Set  $\mathbf{y}^j \leftarrow \mathbf{x} + \mu_j \mathbf{d}$ .
- 22: **end loop**

---

- If  $j = 0$ , then  $\mathbf{x} + \mathbf{d}$  and  $\mathbf{x}$  are contained in the same orthant. In this case, there are no points of nondifferentiability of  $F(\mathbf{x}; \boldsymbol{\epsilon})$  exist on the line segment connecting  $\mathbf{x}$  to  $\mathbf{x} + \mathbf{d}$ . This also means  $\mu_0 = 1$  when reaching line 18. The line-search with backtracking terminates at  $\mathbf{y}^0$ .
- If  $j > 0$ , then line 10– 14 are executed but the condition in line 12 is violated. Notice that  $\mathbf{x} + \mu_B \mathbf{d}$  is on the boundary of the orthant containing  $\mathbf{x}$  and there is also no points of nondifferentiability of  $F(\mathbf{x}; \boldsymbol{\epsilon})$  exist on the line segment connecting  $\mathbf{x}$  to  $\mathbf{x} + \mu_B \mathbf{d}$ . This also means  $\mu_j \geq \xi \mu_B$  when reaching line 16.

In both cases, we end up with a traditional backtracking line-search with  $F(\mathbf{x}; \boldsymbol{\epsilon})$  being  $L_2(\mathbf{x})$ -Lipschitz differentiable in a neighborhood of  $\mathbf{x}$  (e.g., a ball centered at  $\mathbf{x}$  with radius  $\xi \alpha_B \|\mathbf{d}\|$ :  $\mathcal{B}(\mathbf{x}, \xi \mu_B \|\mathbf{d}\|)$ ). Now applying Taylor's Theorem,

$$\begin{aligned} F(\mathbf{x} + \mu \mathbf{d}; \boldsymbol{\epsilon}) &\leq F(\mathbf{x}; \boldsymbol{\epsilon}) + \mu \langle \nabla F(\mathbf{x}; \boldsymbol{\epsilon}), \mathbf{d} \rangle + \frac{1}{2} \mu^2 L_2(\mathbf{x}) \|\mathbf{d}\|^2 \\ &\leq F(\mathbf{x}; \boldsymbol{\epsilon}) + \varpi \mu \langle \nabla F(\mathbf{x}), \mathbf{d} \rangle, \end{aligned}$$

where the second inequality is satisfied for any

$$\mu \in \left( 0, \frac{2(\varpi - 1) \langle \nabla F(\mathbf{x}; \boldsymbol{\epsilon}), \mathbf{d} \rangle}{L_2(\mathbf{x}) \|\mathbf{d}\|^2} \right].$$

Therefore, the backtracking line-search terminates with  $\mu$  that satisfies (41).

Overall, we have demonstrated that SOIR $\ell_1$  is well-posed in the sense that each quadratic subproblem is well-defined (see Lemma 4), and the line-search procedures terminate in a finite number of iterations (see Lemma 2 and Lemma 5).

#### 4 Convergence Analysis

In this section, we present the convergence analysis of the proposed SOIR $\ell_1$ . In the following, we set the tolerance  $\tau = 0$  and hence SOIR $\ell_1$  generates an infinite sequence  $\{\mathbf{x}^k\}_{k \in \mathbb{N}}$ . We first prove the iterates generated by SOIR $\ell_1$  possess the locally stable support property after some finite iteration, meaning  $\mathcal{I}^k$  and  $\mathcal{I}_0^k$  remain unchanged after some  $k \in \mathbb{N}$ .

**Theorem 2** *Let  $\{\mathbf{x}^k\}$  be the sequence generated by Algorithm 1. The following statements hold.*

- (i) *There exists  $\delta > 0$  such that  $|x_i^k| > \delta, i \in \mathcal{I}^k$  holds true for all  $k$ . Consequently,  $\omega_i^k < \hat{\omega} := \lambda p \delta^{p-1}, i \in \mathcal{I}^k$  holds true for all  $k$ .*
- (ii) *There exist index sets  $\mathcal{I}_0^*$  and  $\mathcal{I}^*$  such that  $\mathcal{I}_0^k \equiv \mathcal{I}_0^*$  and  $\mathcal{I}^k \equiv \mathcal{I}^*$  for sufficiently large  $k$ .*
- (iii) *For any cluster point  $\mathbf{x}^*$  of  $\{\mathbf{x}^k\}$ ,  $\mathcal{I}_0(\mathbf{x}^*) = \mathcal{I}_0^*$  and  $\mathcal{I}(\mathbf{x}^*) = \mathcal{I}^*$ .*

*Proof* (i) Suppose by contradiction that this is not true. Then there exist subsequence  $\mathcal{S} \in \mathbb{N}$  and an index  $j \in \mathcal{I}(\mathbf{x}^k)$  such that

$$|\mathcal{S}| = +\infty, \{x_j^k\} \subset \mathbb{R}_{++} \text{ and } \{x_j^k\}_{k \in \mathcal{S}} \rightarrow 0, \quad (42)$$

meaning  $\lim_{\substack{k \rightarrow +\infty \\ k \in \mathcal{S}}} \omega_j^k = +\infty$  and  $\lim_{k \rightarrow +\infty} \epsilon_j^k = 0$ .

We first show that  $x_j^{k+1} = 0$  for all sufficiently large  $k \in \mathcal{S}$ . Notice that index  $j$  is chosen by line 13 in Algorithm 1 infinitely many times. If this were not the case,  $x_j^k$  would remain a positive constant for sufficiently large  $k$ , which would contradict (42).

Suppose now  $j$  is selected by line 13 for sufficiently large  $k \in \mathcal{S}$  such that

$$\mu_{k+1} \omega_j^k \geq \min\{\bar{\mu}, \frac{\xi}{L_f + \alpha}\} \omega_j^k > R + \max\{\bar{\mu}, 1\} L_f \geq |x_j^k - \mu^{k+1} \nabla_j f(\mathbf{x}^k)|. \quad (43)$$

The first inequality of (43) is achieved by (21), and the second inequality is achieved by the argument  $\lim_{\substack{k \rightarrow +\infty \\ k \in \mathcal{S}}} \omega_j^k = +\infty$ , and the third inequality is achieved

$\{\nabla_j f(\mathbf{x}^k)\}$  and  $\{x_j^k\}$  are all bounded over  $\text{Lev}_F$  due to the same arguments presented in Lemma 4 indicated by Assumption 1(i). Here,  $R > 0$  refers to the radius of  $\mathcal{B}(0, R) = \{\mathbf{x} \in \mathbb{R}^n : \|\mathbf{x}\| \leq R\}$  containing  $\text{Lev}_F$ . The last inequality of (43) is achieved by the triangle inequality. By Lemma 7, we know that  $d_i(\mu_{k+1}) = -x_j^k$ . In other words, line 14 returns  $\hat{\mathbf{x}}^{k+1}$  with  $\hat{x}_j^{k+1} = 0$ . This means  $\text{sgn}(\hat{\mathbf{x}}^{k+1}) \neq \text{sgn}(\mathbf{x}^k)$ , so that the QP subproblem is not triggered and  $\mathbf{x}^{k+1} = \hat{\mathbf{x}}^{k+1}$ .

Now consider  $j \in \mathcal{I}_0^{k+1}$ . We show that  $j \in \mathcal{I}_0^k$  for  $\{k+1, k+2, \dots\}$ . This is true since the component  $x_j, j \in \mathcal{I}_0^k$  can only be changed if it is selected by line 10 at some  $\tilde{k} > k$ . However,  $\omega_j^{\tilde{k}} > \omega_j^k$  since  $x_j^k \neq 0, x_j^{\tilde{k}} = 0$  and  $\epsilon_j^{\tilde{k}} = \epsilon_j^{k+1}$ , meaning  $\omega_j^{\tilde{k}} > L_f > |\nabla_j f(\mathbf{x}^k)|$  holds true by (43). This means  $j$  is never selected by line 10, and will remain in  $\mathcal{I}_0^k$  for  $\{k+1, k+2, \dots\}$ —a contradiction with (42).

(ii) Suppose by contradiction this is not true. Then there exists  $j$  and  $\mathbb{N} = \mathcal{S} \cup \mathcal{S}_0$  such that  $|\mathcal{S}| = +\infty, |\mathcal{S}_0| = +\infty, x_j^k \in \mathcal{I}^k, k \in \mathcal{S}$  and  $x_j^k \in \mathcal{I}_0^k, k \in \mathcal{S}_0$ . It then follows from the updating strategy of  $\epsilon$  (lines 6 and 25) that  $\epsilon_j^k$  is reduced for all

$k \in \mathcal{S}$  and hence  $\epsilon_j^k \rightarrow 0$ . Now for sufficiently large  $k \in \mathcal{S}_0$  satisfying  $\omega_j^k > L_f$  and  $[\Psi(\mathbf{x}^k, \boldsymbol{\epsilon}^k)]_j = 0$ . Therefore,  $j$  will never be chosen by line 10 and will stay in  $\mathcal{I}_0^k$  for  $\{k+1, k+2, \dots\}$ , meaning  $|\mathcal{S}| < +\infty$ —a contradiction.

(iii) Obvious. The proof is complete.

#### 4.1 Global convergence

The global convergence of SOIR $\ell_1$  is established in this subsection. For ease of presentation, we first define the following sets of iterations for our analysis.

$$\begin{aligned}\mathcal{S}_\Psi &:= \{k : \mathbf{x}^{k+1} \text{ is obtained from line 11 at the } k\text{th iteration}\}, \\ \mathcal{S}_\Phi &:= \{k : \mathbf{x}^{k+1} \text{ is obtained from line 22 at the } k\text{th iteration}\}, \\ \mathcal{S}_{QP} &:= \{k : \mathbf{x}^{k+1} \text{ is obtained from line 20 at the } k\text{th iteration}\}.\end{aligned}$$

The set  $\mathcal{S}_\Psi$  includes the iterations where an IST subproblem for the current zero components is solved. The set  $\mathcal{S}_\Phi$  includes the iterations where an IST subproblem for the current nonzeros is solved. The set  $\mathcal{S}_{QP}$  includes the iterations where the QP subproblem for the current nonzeros is solved. We further split  $\mathcal{S}_{QP}$  into two subsets based on whether the iterate returned by Algorithm 3 retains the same sign as  $\mathbf{x}^k$ .

$$\begin{aligned}\mathcal{S}_{QP}^N &:= \{k \in \mathcal{S}_{QP} : \text{sgn}(\mathbf{x}^{k+1}) \neq \text{sgn}(\mathbf{x}^k)\}, \\ \mathcal{S}_{QP}^Y &:= \{k \in \mathcal{S}_{QP} : \text{sgn}(\mathbf{x}^{k+1}) = \text{sgn}(\mathbf{x}^k)\}.\end{aligned}$$

By Lemma 5,  $k \in \mathcal{S}_{QP}^N$  means  $\mathbf{x}^{k+1}$  is updated by Algorithm 3 (lines 1–8 or line 9–15), while  $k \in \mathcal{S}_{QP}^Y$  means  $\mathbf{x}^{k+1}$  is updated by Algorithm 3 (lines 16–22).

To show that our algorithm automatically reverts to a second-order method, we first show that the IST update (lines 9–11) is never triggered for sufficiently large  $k$ .

**Theorem 3** *The index sets  $|\mathcal{S}_\Psi| < +\infty$ ,  $|\mathcal{S}_\Phi| < +\infty$  and  $|\mathcal{S}_{QP}^N| < +\infty$ .*

*Proof* If lines 9–11 are executed, then  $|\mathcal{I}^k| < |\mathcal{I}^{k+1}|$  by Lemma 3(i). However, this never happens for sufficiently large  $k$  by Theorem 2. Therefore,  $|\mathcal{S}_\Psi| < \infty$ .

Suppose by contradiction that  $|\mathcal{S}_\Phi| = +\infty$ . It follows from Lemma 2 that for  $k \in \mathcal{S}_\Phi$

$$\begin{aligned}\sum_{k=0}^t [F(\mathbf{x}^k; \boldsymbol{\epsilon}^k) - F(\mathbf{x}^{k+1}; \boldsymbol{\epsilon}^{k+1})] &\geq \sum_{k \in \mathcal{S}_\Phi, k \leq t} [F(\mathbf{x}^k; \boldsymbol{\epsilon}^k) - F(\mathbf{x}^{k+1}; \boldsymbol{\epsilon}^{k+1})] \\ &\geq \sum_{k \in \mathcal{S}_\Phi, k \leq t} [F(\mathbf{x}^k; \boldsymbol{\epsilon}^k) - F(\mathbf{x}^{k+1}; \boldsymbol{\epsilon}^k)] \\ &\geq \frac{\alpha}{2} \sum_{k \in \mathcal{S}_\Phi, k \leq t} \|\mathbf{x}^k - \mathbf{x}^{k+1}\|^2.\end{aligned}$$

Letting  $t \rightarrow \infty$ , we obtain  $\mathbf{d}^k = \mathbf{x}^{k+1} - \mathbf{x}^k \rightarrow \mathbf{0}$ ,  $k \in \mathcal{S}_\Phi$ . There exists  $j \in \mathcal{I}^k$  such that  $\text{sgn}(\hat{x}_j^{k+1}) = \text{sgn}(x_j^k + \mu_k d_j^k) \neq \text{sgn}(x_j^k)$ ,  $k \in \mathcal{S}_\Phi$  by definition. However, by Theorem 2(i), for sufficiently large  $k \in \mathcal{S}_\Phi$ ,  $|\hat{x}_j^k| > \delta \geq 0$ . Therefore,  $\text{sgn}(x_j^k + \mu_k d_j^k) = \text{sgn}(x_j^k)$  for  $|d_j^k| < \frac{\delta}{2\mu}$ , a contradiction. Hence,  $|\mathcal{S}_\Phi| < +\infty$ .

Suppose by contradiction that  $|\mathcal{S}_{\text{QP}}^N| = +\infty$ . By (40),  $\mathcal{I}(\mathbf{x}^{k+1}) \neq \mathcal{I}(\mathbf{x}^k)$  happens for infinitely many times, contradicting Theorem 2(ii). The proof is complete.

We are now ready to prove the global convergence of our proposed algorithm.

**Theorem 4** *Algorithm 1 generates  $\{(\mathbf{x}^k, \boldsymbol{\epsilon}^k)\}$  satisfying  $\lim_{k \rightarrow \infty} \Phi(\mathbf{x}^k, \boldsymbol{\epsilon}^k) = 0$ ,  $\lim_{k \rightarrow \infty} \Psi(\mathbf{x}^k, \boldsymbol{\epsilon}^k) = 0$ , and  $\lim_{k \rightarrow \infty} \boldsymbol{\epsilon}_i^k = 0, i \in \mathcal{I}^k$ . Moreover, there exists  $\hat{k}$  such that  $\boldsymbol{\epsilon}_i^k \equiv \hat{\boldsymbol{\epsilon}}_i^k > 0, i \in \mathcal{I}_0^k$  for all  $k \geq \hat{k}$ . Therefore,  $\lim_{k \rightarrow \infty} \boldsymbol{\epsilon}^k \rightarrow \boldsymbol{\epsilon}^*$  where  $\boldsymbol{\epsilon}_{\mathcal{I}^*}^* = 0$  and  $\boldsymbol{\epsilon}_{\mathcal{I}_0^*}^* = \hat{\boldsymbol{\epsilon}}_{\mathcal{I}_0^*}^*$ .*

*Proof* By 3, there exists  $\hat{k}$  such that  $\{\hat{k}, \hat{k}+1, \dots\} \subset \mathcal{S}_{\text{QP}}^Y$  and line 17 is triggered for any  $k \geq \hat{k}$ . Therefore, it follows that

$$\begin{aligned} F(\mathbf{x}^k; \boldsymbol{\epsilon}^k) - F(\mathbf{x}^{k+1}; \boldsymbol{\epsilon}^{k+1}) &\geq F(\mathbf{x}^k; \boldsymbol{\epsilon}^k) - F(\mathbf{x}^{k+1}; \boldsymbol{\epsilon}^k) \\ &\geq -\varpi\mu^k \langle \nabla_{\mathcal{W}_k} F(\mathbf{x}^k; \boldsymbol{\epsilon}^k), \mathbf{d}_{\mathcal{W}}^k \rangle \\ &\geq \frac{2\varpi\xi(1-\varpi) |\langle \nabla_{\mathcal{W}_k} F(\mathbf{x}^k; \boldsymbol{\epsilon}^k), \bar{\mathbf{d}}^k \rangle|^2}{\bar{\lambda}_{\max} \|\bar{\mathbf{d}}^k\|^2} \quad (44) \\ &\geq \frac{\varpi\xi(1-\varpi)\bar{\lambda}_{\min}^2}{2\bar{\lambda}_{\max}^3} \|\nabla_{\mathcal{W}_k} F(\mathbf{x}^k; \boldsymbol{\epsilon}^k)\|^2, \end{aligned}$$

where the third inequality is by (41) and the last inequality is by (35) and 33.

This, combined with (16), yields that for  $k \geq \hat{k}, k \in \mathcal{S}_{\text{QP}}^Y$

$$\begin{aligned} F(\mathbf{x}^k, \boldsymbol{\epsilon}^k) - F(\mathbf{x}^{k+1}, \boldsymbol{\epsilon}^{k+1}) &\geq \frac{\varpi\xi(1-\varpi)\bar{\lambda}_{\min}^2}{2\bar{\lambda}_{\max}^3} \|[\Phi^k]_{\mathcal{W}_k}\|^2 \\ &\geq \frac{\eta_{\Phi}\varpi\xi(1-\varpi)\bar{\lambda}_{\min}^2}{2\bar{\lambda}_{\max}^3} \|[\Phi^k]_{\mathcal{I}^k}\|^2 \quad (45) \\ &= \frac{\eta_{\Phi}\varpi\xi(1-\varpi)\bar{\lambda}_{\min}^2}{2\bar{\lambda}_{\max}^3} \|\Phi^k\|^2, \end{aligned}$$

where the last inequality is by line 13 of 1 and the equality is by the definition of  $\Phi$ . Summing up both sides from  $\hat{k}$  to  $t$  and letting  $t \rightarrow \infty$ , we immediately have  $\|\Phi^k\| \rightarrow 0$ .

On the other hand, since  $\{\hat{k}, \hat{k}+1, \dots\} \subset \mathcal{S}_{\text{QP}}^Y$ ,  $\|\Psi^k\| < \gamma\|\Phi^k\|$  is satisfied for all  $k \geq \hat{k}$ . Therefore,  $\|\Psi^k\| \rightarrow 0$ .

Finally, 2 immediately implies that  $\boldsymbol{\epsilon}_i^k \rightarrow 0, i \in \mathcal{I}^k$  and  $\boldsymbol{\epsilon}_i^k \equiv \hat{\boldsymbol{\epsilon}}_i^k > 0, i \in \mathcal{I}_0^k$  for all  $k \geq \hat{k}$ .

This result implies that for all  $k \geq \hat{k}$ ,  $(\mathbf{x}^k, \boldsymbol{\epsilon}^k)$  always stays in the reduced subspace

$$\mathcal{M}(\mathbf{x}^*, \boldsymbol{\epsilon}^*) := \{\mathbf{x} \mid \mathbf{x}_{\mathcal{I}_0^*} = 0, \boldsymbol{\epsilon}_{\mathcal{I}_0^*} \equiv \hat{\boldsymbol{\epsilon}}_{\mathcal{I}_0^*}^*\},$$

and  $\mathbf{x}^k$  is contained in the reduced subspace

$$\overline{\mathcal{M}}(\mathbf{x}^*) := \{\mathbf{x} \mid \mathbf{x}_{\mathcal{I}_0^*} = 0\}.$$

We also have from 4 the local equivalence between  $\Phi$  and the subspace gradient of  $F(\mathbf{x}; \boldsymbol{\epsilon})$ .

**Corollary 1** For sufficiently large  $k$ ,  $\Phi_i^k = \nabla_i F(\mathbf{x}^k; \boldsymbol{\epsilon}^k), i \in \mathcal{I}^*$ . Therefore,

$$\lim_{k \rightarrow \infty} \nabla_{\mathcal{I}^*} F(\mathbf{x}^k; \boldsymbol{\epsilon}^k) = 0.$$

*Proof* This is obvious that we only have to take care of the second and third cases in the definition of  $\Phi$ . For  $i \in \mathcal{I}_+^k$  and  $\nabla_i f(\mathbf{x}^k) + \omega_i^k > 0$ , 2 implies that  $\max\{x_i^k, \nabla_i f(\mathbf{x}^k) - \omega_i^k\} > \delta > 0$ . However,  $\Phi_i^k \rightarrow 0$  by 4. This implies that  $\Phi_i^k = \nabla_i f(\mathbf{x}^k) + \omega_i = \nabla_i F(\mathbf{x}^k; \boldsymbol{\epsilon}^k)$  for all sufficiently large  $k$ .

For  $i \in \mathcal{I}_-^k$  and  $\nabla_i f(\mathbf{x}^k) - \omega_i^k < 0$ , same argument also yields that  $\Phi_i^k = \nabla_i f(\mathbf{x}^k) + \omega_i = \nabla_i F(\mathbf{x}^k; \boldsymbol{\epsilon}^k)$  for all sufficiently large  $k$ .

#### 4.2 Convergence rate under KL property

The Kurdyka-Łojasiewicz (KL) property is widely used to analyze the convergence rate of an algorithm under the assumption that this property is satisfied at the optimal solution. For example, [38] have proved a series of convergence results of descent methods for semi-algebraic problems by assuming that the objective satisfies the KL property. This property, which covers a wide range of problems such as nonsmooth semi-algebraic minimization problem [39], is given below.

**Definition 2 (Kurdyka-Łojasiewicz property)** The function  $f : \mathbb{R}^n \rightarrow \mathbb{R} \cup \{+\infty\}$  is said to have the Kurdyka-Łojasiewicz property at  $\mathbf{x}^* \in \text{dom} \bar{\partial} f$  if there exists  $\varsigma \in (0, +\infty]$ , a neighborhood  $U$  of  $\mathbf{x}^*$  and a continuous concave function  $\phi : [0, \varsigma) \rightarrow \mathbb{R}_+$  such that:

- (i)  $\phi(0) = 0$ ,
- (ii)  $\phi$  is  $C^1$  on  $(0, \varsigma)$ ,
- (iii) for all  $s \in (0, \varsigma)$ ,  $\phi'(s) > 0$ ,
- (iv) for all  $\mathbf{x}$  in  $U \cap [f(\mathbf{x}^*) < f < f(\mathbf{x}^*) + \varsigma]$ , the Kurdyka-Łojasiewicz inequality holds

$$\phi'(f(\mathbf{x}) - f(\mathbf{x}^*)) \text{dist}(0, \bar{\partial} f(\mathbf{x})) \geq 1.$$

Generally,  $\phi$  takes the form  $\phi(s) = cs^{1-\theta}$  for some  $\theta \in [0, 1)$  and  $c > 0$ . If  $f$  is smooth, then condition (iv) reverts to

$$\|\nabla(\phi \circ f)(\mathbf{x})\| \geq 1.$$

$\theta$  is known as the KL exponent, which is defined as follows.

**Definition 3 (KL exponent)** For a proper closed function  $f$  satisfying the KL property at  $\bar{\mathbf{x}} \in \text{dom } \partial f$ , if the corresponding function  $\phi$  can be chosen as  $\phi(s) = cs^{1-\theta}$  for some  $c > 0$  and  $\theta \in [0, 1)$ , i.e., there exist  $c, \rho > 0$  and  $\varsigma \in (0, \infty]$  so that

$$\text{dist}(0, \partial f(\mathbf{x})) \geq c(f(\mathbf{x}) - f(\bar{\mathbf{x}}))^\theta$$

whenever  $\|\mathbf{x} - \bar{\mathbf{x}}\| \leq \rho$  and  $f(\bar{\mathbf{x}}) < f(\mathbf{x}) < f(\bar{\mathbf{x}}) + \varsigma$ , then we say that  $f$  has the KL property at  $\bar{\mathbf{x}}$  with an exponent of  $\theta$ . If  $f$  is a KL function and has the same exponent  $\theta$  at any  $\bar{\mathbf{x}} \in \text{dom } \partial f$ , then we say that  $f$  is a KL function with an exponent of  $\theta$ .

By 2 and 4,  $x_i^k \equiv 0, \epsilon_i^k \equiv \epsilon_i^{\hat{k}}, i \in \mathcal{I}_0^*$  for any  $k \geq \hat{k}$ , and the iterates  $\{x_{\mathcal{I}}^*\}_{k \geq \hat{k}}$  remains in the interior of subspace  $\mathbb{R}^{\mathcal{I}^*}$ . Therefore, we can consider  $F(\mathbf{x}; \boldsymbol{\epsilon})$  as a function in the interior of subspace  $\mathbb{R}^{\mathcal{I}^*}$ . Moreover, we write  $\boldsymbol{\epsilon} = \boldsymbol{\epsilon} \circ \boldsymbol{\epsilon}$  and treat  $\boldsymbol{\epsilon}$  also as a variable, i.e.,  $F(\mathbf{x}; \boldsymbol{\epsilon}) = F(\mathbf{x}, \boldsymbol{\epsilon})$ .

As noted in [40, Page 63, Section 2.1], the KL exponent of a given function is often extremely hard to determine or estimate. The most useful and related result is the following theorem given in [41] and its thorough proof is provided in [15, Theorem 7]. It claims that a smooth function has KL exponent  $\theta = 1/2$  at a nondegenerate critical point (critical point with nonsingular Hessian). Therefore, we can have the following result.

**Proposition 3** Consider the following four cases.

- (a) The KL exponent of  $F(\mathbf{x}, \boldsymbol{\epsilon})$  restricted on  $\mathcal{M}(\mathbf{x}^*, \boldsymbol{\epsilon}^*)$  at  $(x_{\mathcal{I}^*}^*, 0)$  is  $\theta$ .
- (b) The KL exponent of  $F(\mathbf{x}, \boldsymbol{\epsilon})$  at  $(\mathbf{x}^*, 0)$  is  $\theta$ .
- (c) The KL exponent of  $F(\mathbf{x})$  restricted on  $\overline{\mathcal{M}}(\mathbf{x}^*)$  at  $x_{\mathcal{I}^*}^*$  is  $\theta$ .
- (d) The KL exponent of  $F(\mathbf{x})$  at  $\mathbf{x}^*$  is  $\theta$ .

We have (a)  $\implies$  (b), (c)  $\implies$  (d), and (a)  $\implies$  (c). Morevoer, we have  $\theta \in (0, 1)$  and  $\theta = 1/2$  if  $\nabla_{\mathcal{I}^*}^2 F(\mathbf{x}^*)$  in (c).

*Proof* (a)  $\implies$  (b) and (c)  $\implies$  (d) can be directly derived by [42, Theorem 3.7].

To prove (a)  $\implies$  (c), note that  $\boldsymbol{\epsilon}_{\mathcal{I}^*}^* = 0$  and  $\nabla_{\boldsymbol{\epsilon}_{\mathcal{I}^*}} F(\mathbf{x}^*, \boldsymbol{\epsilon}^*) = 2\omega_{\mathcal{I}^*}^* \circ \boldsymbol{\epsilon}_{\mathcal{I}^*}^* = 0$ . By the definition of KL exponent and (i), there exists  $c > 0$  such that

$$\|\nabla_{\mathcal{I}^*} F(\mathbf{x})\| = \|\nabla_{(\mathbf{x}_{\mathcal{I}^*}, \boldsymbol{\epsilon}_{\mathcal{I}^*})} F(\mathbf{x}, \boldsymbol{\epsilon})\| \geq c(F(\mathbf{x}, \boldsymbol{\epsilon}) - F(\mathbf{x}^*, \boldsymbol{\epsilon}^*))^\theta \geq c(F(\mathbf{x}) - F(\mathbf{x}^*))^\theta,$$

meaning (c) is also true.

Moreover, if  $\nabla_{\mathcal{I}^*}^2 F(\mathbf{x}^*)$ , [15, Theorem 7] indicates that the KL exponent of (c) is  $1/2$ . In addition,  $\|\nabla_{\mathcal{I}^*} F(\mathbf{x})\| \geq c(F(\mathbf{x}) - F(\mathbf{x}^*))^0$  cannot be true, so that  $\theta \neq 0$ .

Convergence rate analysis of iteratively reweighted methods for nonconvex regularization problems ( $\mathcal{P}$ ) under KL property was completed in [14][15]. In [38][43][42], the general convergence rate analysis framework is given for a wide range of descent methods.

**Lemma 6** (Prototypical result on convergence rate [42]) For a certain algorithm of interest, consider a suitable potential function. Suppose that the potential function satisfies the KL property with an exponent of  $\theta \in (0, 1)$ , and that  $\{\mathbf{x}^k\}$  is a bounded sequence generated by the algorithm. Then the following results hold.

- (i) If  $\theta = 0$ , then  $\{\mathbf{x}^k\}$  converges finitely.
- (ii) If  $\theta \in (0, \frac{1}{2}]$ , then  $\{\mathbf{x}^k\}$  converges locally linearly.
- (iii) If  $\theta \in (\frac{1}{2}, 1)$ , then  $\{\mathbf{x}^k\}$  converges locally sublinearly.

We proceed to show our algorithm also satisfies the “sufficient decrease condition” and the “relative error condition” given by [38][43][44]. Then the analysis is standard and can be derived following the same analysis.

**Theorem 5** Let  $\{\mathbf{x}^k\}$  be a sequence generated by 1 and  $F(\mathbf{x}, \boldsymbol{\epsilon})$  restricted on  $\mathcal{M}(\mathbf{x}^*, \boldsymbol{\epsilon}^*)$  is a KL function at all stationary point  $(\mathbf{x}^*, \mathbf{0})$  with  $\mathcal{I}(\mathbf{x}^*) = \mathcal{I}^*$  and  $\nabla_{\mathcal{I}^*} F(\mathbf{x}^*; \mathbf{0}) = 0$ . Then  $\{\mathbf{x}^k\}$  converges to a stationary point  $\mathbf{x}^*$  of  $F(\mathbf{x})$  and

$$\sum_{k=0}^{\infty} \|\mathbf{x}^{k+1} - \mathbf{x}^k\|_2 < \infty. \quad (46)$$

Moreover, assume that  $F$  is a KL function with  $\phi$  in the KL definition taking the form  $\phi(s) = cs^{1-\theta}$  for some  $\theta \in [0, 1)$  and  $c > 0$ . Then the following statements hold.

(i) If  $\theta \in (0, \frac{1}{2}]$ , then there exist  $\vartheta \in (0, 1)$ ,  $c_1 > 0$  such that

$$\|\mathbf{x}^k - \mathbf{x}^*\|_2 < c_1 \vartheta^k \quad (47)$$

for sufficiently large  $k$ ;

(ii) If  $\theta \in (\frac{1}{2}, 1)$ , then there exist  $c_2 > 0$  such that

$$\|\mathbf{x}^k - \mathbf{x}^*\|_2 < c_2 k^{-\frac{1-\theta}{2\theta-1}} \quad (48)$$

for sufficiently large  $k$ .

*Proof* For brevity and without loss of generality, we remove the subscript  $\mathcal{I}^*$  in the remaining part of this subsection. It follows from (44) and (36) that

$$F(\mathbf{x}^{k+1}; \boldsymbol{\epsilon}^{k+1}) \leq F(\mathbf{x}^{k+1}; \boldsymbol{\epsilon}^k) \leq F(\mathbf{x}^k; \boldsymbol{\epsilon}^k) - \frac{2\varpi\xi(1-\varpi)\lambda_{\min}}{2\bar{\lambda}_{\max}^3} \|\mathbf{x}^{k+1} - \mathbf{x}^k\|^2.$$

which gives

$$F(\mathbf{x}^{k+1}, \boldsymbol{\epsilon}^{k+1}) + C_1 \|\mathbf{x}^{k+1} - \mathbf{x}^k\|^2 \leq F(\mathbf{x}^k, \boldsymbol{\epsilon}^k), \quad (49)$$

where  $C_1 = \frac{2\varpi\xi(1-\varpi)\bar{\lambda}_{\min}}{2\bar{\lambda}_{\max}^3}$ . Therefore, the sufficient decrease condition holds true for  $F(\mathbf{x}, \boldsymbol{\epsilon})$ .

Next, consider the upper bound for  $\|\nabla_{\mathbf{x}} F(\mathbf{x}^{k+1}, \boldsymbol{\epsilon}^{k+1})\|$ .

$$\begin{aligned} \|\nabla_{\mathbf{x}} F(\mathbf{x}^{k+1}, \boldsymbol{\epsilon}^{k+1})\| &\leq \|\nabla_{\mathbf{x}} F(\mathbf{x}^{k+1}, \boldsymbol{\epsilon}^{k+1}) - \nabla_{\mathbf{x}} F(\mathbf{x}^k, \boldsymbol{\epsilon}^k)\| + \|\nabla_{\mathbf{x}} F(\mathbf{x}^k, \boldsymbol{\epsilon}^k)\| \\ &\leq \|\nabla f(\mathbf{x}^{k+1}) - \nabla f(\mathbf{x}^k)\| + \|\boldsymbol{\omega}(\mathbf{x}^{k+1}, (\boldsymbol{\epsilon}^{k+1})^2) - \boldsymbol{\omega}(\mathbf{x}^k, (\boldsymbol{\epsilon}^k)^2)\| + \|\nabla_{\mathbf{x}} F(\mathbf{x}^k, \boldsymbol{\epsilon}^k)\| \end{aligned} \quad (50)$$

By the Lipschitz property of  $f$ , the first term in is bounded by

$$\|\nabla f(\mathbf{x}^{k+1}) - \nabla f(\mathbf{x}^k)\| \leq L \|\mathbf{x}^{k+1} - \mathbf{x}^k\|$$

Now we give an upper bound for the third term. Combining (41), (35) and (36), we have for  $k \geq \hat{k}$ ,

$$\|\mathbf{x}^{k+1} - \mathbf{x}^k\| = \|\mu^k \bar{\mathbf{d}}^k\| \geq \frac{2\xi(1-\varpi)|\langle \mathbf{g}^k, \bar{\mathbf{d}}^k \rangle|}{L_F \|\bar{\mathbf{d}}^k\|^2} \frac{\|\mathbf{g}^k\|}{\bar{\lambda}_{\max}} \geq \frac{\xi(1-\varpi)\bar{\lambda}_{\min}^2}{2L_F \bar{\lambda}_{\max}^2} \|\nabla_{\mathbf{x}} F(\mathbf{x}^k, \boldsymbol{\epsilon}^k)\|.$$

Finally, we give an upper bound for the second term. From [15, lemma 1], we have the change between  $\boldsymbol{\omega}(\mathbf{x}^{k+1}, (\boldsymbol{\epsilon}^{k+1})^2)$  and  $\boldsymbol{\omega}(\mathbf{x}^k, (\boldsymbol{\epsilon}^k)^2)$  is bounded by,

$$\|\boldsymbol{\omega}(\mathbf{x}^{k+1}, (\boldsymbol{\epsilon}^{k+1})^2) - \boldsymbol{\omega}(\mathbf{x}^k, (\boldsymbol{\epsilon}^k)^2)\| \leq C[\sqrt{|\mathcal{I}^*|} \|\mathbf{x}^{k+1} - \mathbf{x}^k\|_2 + 2\|\boldsymbol{\epsilon}^0\|_{\infty} (\|\boldsymbol{\epsilon}^k\|_1 - \|\boldsymbol{\epsilon}^{k+1}\|_1)]$$

where  $\bar{C} := \lambda p(1-p)(\delta)^{p-2}$ . Putting together the bounds for all three terms, we have

$$\begin{aligned} \|\nabla_{\mathbf{x}} F(\mathbf{x}^{k+1}, \boldsymbol{\varepsilon}^{k+1})\| \leq & (L + \frac{2L_F \bar{\lambda}_{\max}^2}{\xi(1-\varpi)\bar{\lambda}_{\min}^2} + \bar{C}\sqrt{|\mathcal{I}^*|})\|\mathbf{x}^{k+1} - \mathbf{x}^k\|_2 \\ & + 2\|\boldsymbol{\varepsilon}^0\|_\infty \bar{C}(\|\boldsymbol{\varepsilon}^k\|_1 - \|\boldsymbol{\varepsilon}^{k+1}\|_1) \end{aligned} \quad (51)$$

On the other hand,

$$\begin{aligned} \|\nabla_{\boldsymbol{\varepsilon}} F(\mathbf{x}^{k+1}, \boldsymbol{\varepsilon}^{k+1})\| \leq & \|\nabla_{\boldsymbol{\varepsilon}} F(\mathbf{x}^{k+1}, \boldsymbol{\varepsilon}^{k+1})\|_1 = \sum_{i \in \mathcal{I}^*} 2[\omega(\mathbf{x}^{k+1}, (\boldsymbol{\varepsilon}^{k+1})^2)]_i \cdot \varepsilon_i^{k+1} \\ \leq & \sum_{i \in \mathcal{I}^*} 2\hat{\omega} \frac{\sqrt{\beta}}{1-\sqrt{\beta}} (\varepsilon_i^k - \varepsilon_i^{k+1}) \leq 2\hat{\omega} \frac{\sqrt{\beta}}{1-\sqrt{\beta}} (\|\boldsymbol{\varepsilon}^k\|_1 - \|\boldsymbol{\varepsilon}^{k+1}\|_1) \end{aligned} \quad (52)$$

where the second inequality is by 2 and  $\boldsymbol{\varepsilon}^{k+1} \leq \sqrt{\beta}\boldsymbol{\varepsilon}^k$ . Overall, we obtain from (51) and (52) that

$$\|\nabla F(\mathbf{x}^{k+1}, \boldsymbol{\varepsilon}^{k+1})\| \leq C_2(\|\mathbf{x}^{k+1} - \mathbf{x}^k\| + \|\boldsymbol{\varepsilon}^k\|_1 - \|\boldsymbol{\varepsilon}^{k+1}\|_1) \quad (53)$$

with

$$C_2 := \max\{L + \frac{2L_F \bar{\lambda}_{\max}^2}{\xi(1-\varpi)\bar{\lambda}_{\min}^2} + \bar{C}\sqrt{|\mathcal{I}^*|}, 2\|\boldsymbol{\varepsilon}^0\|_\infty \bar{C} + 2\hat{\omega} \frac{\sqrt{\beta}}{1-\sqrt{\beta}}\}.$$

Therefore, the relative error condition holds true for  $F(\mathbf{x}, \boldsymbol{\varepsilon})$ .

The proof of (46) essentially follows that of the convergence analysis of [38, Theorem 2.9] or [43, Theorem 4]. The convergence rate can be derived following the same argument in the analysis of [14, Theorem 10] or [15, Theorem 10]. Therefore, the rest proof is omitted.

### 4.3 Local convergence for exact QP solution

We consider the local convergence of 1 in the neighborhood of critical points satisfying certain assumptions, delineated below. For the most part, our assumptions in this subsection represent the local convexity near a critical point and the exact solution of the QP subproblem. Since we focus on the local behavior, we only consider the iterates with  $k \geq \hat{k}$ , so that the algorithm reverts to solving a QP subproblem combined with a backtracking line-search. Specifically, we assume the following additional assumptions in this subsection.

**Assumption 6** Suppose  $\{\mathbf{x}^k\}$  is generated by 1 with  $\{\mathbf{x}^k\} \rightarrow \mathbf{x}^*$ . For all  $k \geq \hat{k}$ , the following holds true.

- (i)  $f$  is twice continuously differentiable. The subspace Hessian of  $F(\mathbf{x})$  at  $\mathbf{x}^*$  is invertible with  $\|\nabla_{\mathcal{I}^* \mathcal{I}^*}^2 F(\mathbf{x}^*)^{-1}\| < M$ .
- (ii) Exact Hessian  $\mathbf{H}^k = \nabla_{\mathcal{I}^k \mathcal{I}^k}^2 F(\mathbf{x}^k; \boldsymbol{\varepsilon}^k)$  is used in  $m_k(d)$  and  $\mathcal{W}_k \equiv \mathcal{I}^k$ .
- (iii) QP subproblem (32) is solved exactly  $\bar{\mathbf{d}}^k = (\mathbf{H}^k)^{-1} \mathbf{g}^k$ .
- (iv) For all sufficiently large  $k$ , unit stepsize  $\mu_k \equiv 1$  is accepted.

Notice that  $\nabla_{\mathcal{I}^* \mathcal{I}^*}^2 F(\mathbf{x})$  is locally Lipschitz continuous near  $\mathbf{x}^*$  with constant  $L_H$ . In the previous subsection, if  $\nabla_{\mathcal{I}^* \mathcal{I}^*}^2 F(\mathbf{x})$  is invertible, 3 implies the KL exponent of  $F$  is  $1/2$  at  $\mathbf{x}^*$ . Therefore, superlinear convergence rate is achieved by 5. However, in the following, we show that second-order convergence rate can be reached if 6 is satisfied and  $\epsilon_{\mathcal{I}^*}^k$  is locally driven to 0 at a second-order speed.

**Theorem 7** *There exists a subspace neighborhood of  $\mathbf{x}^*$ , so that  $\forall k \geq k_1$*

$$\|\mathbf{x}^{k+1} - \mathbf{x}^*\| \leq \frac{3ML_H}{2} \|\mathbf{x}^k - \mathbf{x}^*\|^2 + \mathcal{O}(\|\epsilon\|). \quad (54)$$

*Proof* Since we are now working in the subspace  $\mathbb{R}^{\mathcal{I}^*}$ , we remove the subscript  $\mathcal{W}_k$  for simplicity. Given  $\nabla^2 F(\mathbf{x}^*)$  is nonsingular, we can select sufficiently small  $\rho$  so that  $\nabla^2 F(\mathbf{x}^k; \epsilon^k)$  is also nonsingular for any  $\|\mathbf{x}^k - \mathbf{x}^*\| < \rho$  and  $\|\epsilon^k\| < \rho$ , since  $\nabla^2 F(\mathbf{x}^k; \epsilon^k)$  is continuous with  $\epsilon$ . Therefore, we have

$$\begin{aligned} \mathbf{x}^{k+1} - \mathbf{x}^* &= \mathbf{x}^k - \mathbf{x}^* - \nabla^2 F(\mathbf{x}^k; \epsilon^k)^{-1} \nabla F(\mathbf{x}^k; \epsilon^k) \\ &= \mathbf{x}^k - \mathbf{x}^* - \nabla^2 F(\mathbf{x}^k; \epsilon^k)^{-1} (\nabla F(\mathbf{x}^k; \epsilon^k) - \nabla F(\mathbf{x}^*)) \\ &= \nabla^2 F(\mathbf{x}^k; \epsilon^k)^{-1} (\nabla F(\mathbf{x}^*) - \nabla F(\mathbf{x}^k; \epsilon^k) - \nabla^2 F(\mathbf{x}^k; \epsilon^k)(\mathbf{x}^* - \mathbf{x}^k)). \end{aligned}$$

Hence, we have

$$\begin{aligned} \|\mathbf{x}^{k+1} - \mathbf{x}^*\| &\leq \|\nabla^2 F(\mathbf{x}^k; \epsilon^k)^{-1}\| \|\nabla F(\mathbf{x}^*) - \nabla F(\mathbf{x}^k; \epsilon^k) - \nabla^2 F(\mathbf{x}^k; \epsilon^k)(\mathbf{x}^* - \mathbf{x}^k)\| \\ &\leq \|\nabla^2 F(\mathbf{x}^k; \epsilon^k)^{-1}\| \|\nabla F(\mathbf{x}^*) - \nabla F(\mathbf{x}^k) - \nabla^2 F(\mathbf{x}^k)(\mathbf{x}^* - \mathbf{x}^k) \\ &\quad + \|\nabla F(\mathbf{x}^k) - \nabla F(\mathbf{x}^k; \epsilon^k) + [\nabla^2 F(\mathbf{x}^k) - \nabla^2 F(\mathbf{x}^k; \epsilon^k)](\mathbf{x}^* - \mathbf{x}^k)\|. \end{aligned} \quad (55)$$

We then take care each part of the inequality separately.

First, we can consider even smaller  $\rho > 0$  and  $\mathbf{x}^k$  satisfying  $\|\mathbf{x}^k - \mathbf{x}^*\| \leq \rho < \frac{1}{2ML_F}$  (of course, this means the associated  $\epsilon^k$  is also smaller). Since  $\nabla^2 F(\mathbf{x}^*)$  is non-singular,

$$\begin{aligned} \|\nabla^2 F(\mathbf{x}^*)^{-1} (\nabla^2 F(\mathbf{x}^k) - \nabla^2 F(\mathbf{x}^*))\| &\leq \|\nabla^2 F(\mathbf{x}^*)^{-1}\| \|\nabla^2 F(\mathbf{x}^k) - \nabla^2 F(\mathbf{x}^*)\| \\ &\leq ML_H \|\mathbf{x}^k - \mathbf{x}^*\| \leq \rho ML_H \leq \frac{1}{2}. \end{aligned}$$

Therefore  $\nabla^2 F(\mathbf{x}^k)$  is also nonsingular and

$$\|\nabla^2 F(\mathbf{x}^k)^{-1}\| \leq \frac{\|\nabla^2 F(\mathbf{x}^*)^{-1}\|}{1 - \|\nabla^2 F(\mathbf{x}^*)^{-1} (\nabla^2 F(\mathbf{x}^k) - \nabla^2 F(\mathbf{x}^*))\|} \leq 2M.^1$$

We can then choose  $\rho$  even smaller so that

$$\|\nabla^2 F(\mathbf{x}^k; \epsilon^k)^{-1}\| < 3M \quad (56)$$

for any  $\|\mathbf{x}^k - \mathbf{x}^*\| < \rho$  and  $\|\epsilon^k\| < \rho$ , since  $\nabla^2 F(\mathbf{x}^k; \epsilon^k)^{-1}$  is continuous with  $\epsilon$ .

Second, we have that there exists  $\hat{x}_i^k$  satisfying  $|\hat{x}_i^k| \in (|x_i^k|, |x_i^k| + \epsilon_i^k)$  and

$$|\lambda p(|x_i^k|)^{p-1} - \lambda p(|x_i^k| + \epsilon_i^k)^{p-1}| = \lambda p(p-1) |\hat{x}_i^k|^{p-2} \epsilon_i^k \leq \lambda p(p-1) \delta^{p-2} \epsilon_i^k,$$

<sup>1</sup> For matrix  $A, B$ , if  $A$  is nonsingular and  $\|A^{-1}(B - A)\|_2 < 1$ , then  $B$  is nonsingular and  $\|B^{-1}\|_2 \leq \frac{\|A^{-1}\|_2}{1 - \|A^{-1}(B - A)\|_2}$ .

where  $\delta$  is defined as 2. Therefore, it holds that

$$\|\nabla F(\mathbf{x}^k) - \nabla F(\mathbf{x}^k; \boldsymbol{\epsilon}^k)\| \leq \lambda p(1-p)\delta^{p-2}\|\boldsymbol{\epsilon}^k\|. \quad (57)$$

On the other hand, we have that there exists  $\hat{x}_i^k$  satisfying  $|\hat{x}_i^k| \in (|x_i^k|, |x_i^k| + \epsilon_i^k)$  and

$$\begin{aligned} |\lambda p(p-1)(|x_i^k|)^{p-2} - (|x_i^k| + \epsilon_i^k)^{p-2}| &= \lambda p(p-1)(p-2)|\hat{x}_i^k|^{p-3}\epsilon_i^k \\ &\leq \lambda p(p-1)(p-2)\delta^{p-3}\epsilon_i^k, \end{aligned}$$

where  $\delta$  is defined as 2. Therefore, it holds that

$$\|\nabla^2 F(\mathbf{x}^k) - \nabla^2 F(\mathbf{x}^k; \boldsymbol{\epsilon}^k)\| \leq \lambda p(p-1)(p-2)\delta^{p-3}\|\boldsymbol{\epsilon}^k\|,$$

implying

$$\begin{aligned} \|[\nabla^2 F(\mathbf{x}^k) - \nabla^2 F(\mathbf{x}^k; \boldsymbol{\epsilon}^k)](\mathbf{x}^* - \mathbf{x}^k)\| &\leq \|\nabla^2 F(\mathbf{x}^k) - \nabla^2 F(\mathbf{x}^k; \boldsymbol{\epsilon}^k)\| \|\mathbf{x}^* - \mathbf{x}^k\| \\ &\leq \lambda p(p-1)(p-2)\delta^{p-3}\|\boldsymbol{\epsilon}^k\| \|\mathbf{x}^* - \mathbf{x}^k\|. \end{aligned} \quad (58)$$

Finally,  $\nabla F(\mathbf{x})$  is twice continuously differentiable near  $\mathbf{x}^*$  by 6, so

$$\|\nabla F(\mathbf{x}^*) - \nabla F(\mathbf{x}^k) - \nabla^2 F(\mathbf{x}^k)(\mathbf{x}^* - \mathbf{x}^k)\| = \frac{L_H}{2}\|\mathbf{x}^k - \mathbf{x}^*\|^2. \quad (59)$$

Now we can continue with (55) combined with (56), (57), (58) and (59) and have for all  $\|\mathbf{x}^k - \mathbf{x}^*\| < \rho$  and  $\|\boldsymbol{\epsilon}^k\| < \rho$  that

$$\begin{aligned} \|\mathbf{x}^{k+1} - \mathbf{x}^*\| &\leq 3M\left(\frac{L_H}{2}\|\mathbf{x}^k - \mathbf{x}^*\|^2 + \lambda p(1-p)\delta^{p-2}\|\boldsymbol{\epsilon}^k\| \right. \\ &\quad \left. + \lambda p(p-1)(p-2)\delta^{p-3}\|\boldsymbol{\epsilon}^k\| \|\mathbf{x}^* - \mathbf{x}^k\|\right) \\ &\leq \frac{3ML_H}{2}\|\mathbf{x}^k - \mathbf{x}^*\|^2 + \mathcal{O}(\|\boldsymbol{\epsilon}\|). \end{aligned}$$

## 5 Variants and Extensions

We discuss possible variants of QP subproblems and the extension of our algorithm to general nonconvex regularizers.

### 5.1 Variants of the QP subproblem

The QP subproblem solved in line 16–20 seek a (inexact) Newton direction within the same orthant that can cause a decrease in  $F(\mathbf{x}, \boldsymbol{\epsilon})$ . The global convergence guarantees the QP subproblem will be triggered for every iteration after some  $\hat{k}$ . In fact, many other QP subproblems can be a substitute, and the same properties will still be maintained as long as it generates a sufficient decrease in the objective. As an example, we can replace line 16–20 with the trust region Newton subproblem which is proposed in [45] and is shown to converge to second-order optimal solution.

The major difference of this subproblem and the original include: (i) the subproblem can accept nonconvex  $\mathbf{H}^k$ , though this requires a nonconvex QP subproblem solver. Please see [45] for efficient subproblem solvers. (ii) If the QP yields a

direction leading out of the current orthant, then the new iterate is accepted as long as it causes decrease in  $F(\mathbf{x}, \epsilon)$ ; otherwise the trust-region radius is reduced. (iii) If the QP yields a direction to stay in the current orthant, then a classic trust-region update is executed.

One can follow the same analysis to obtain results such as 2 and 4, which are skipped here. The algorithm then locally reverts to the one presented in [45]. A similar convergence rate and convergence to a second-order optimal solution can also be derived. Due to space limitations, we will not delve into the details of that topic. The key point here is that the proposed algorithmic framework can potentially incorporate many variants of QP subproblems and locally revert to classic second-order methods.

## 5.2 Extension to general nonconvex regularization

In this section, we extend our method to solve the generic nonconvex regularized sparse optimization Problems 1, the approximated local model can be formulated as,

$$\underset{\mathbf{x} \in \mathbb{R}^n}{\text{minimize}} \quad G_k(\mathbf{x}) := f(\mathbf{x}) + \sum_{i=1}^n \omega_i^k |x_i|, \quad (60)$$

where  $\omega_i^k = r'(|x_i^k| + \epsilon_i^k)$ . There is a class of approximations to  $\ell_0$  norm problem that can be expressed in such form, see 1. If  $r'(0^+) < \infty$ , we can alternatively set  $\epsilon_i^k \equiv 0$ . The prescribed parameter  $q$  in these models needs to be set appropriately, to ensure all the analysis we have derived is still valid.

**Assumption 8** *On the level set  $\text{Lev}_F$  described in lemma 4, the following condition holds  $|\nabla_i f(\mathbf{x})| < r'(0^+)$ .*

This condition appears in many nonsmooth optimization algorithms and generally takes the form  $0 \in \text{rint} \partial f(\mathbf{x})$  for minimizing  $f$ . In our case, this condition can be satisfied by setting  $p$  in the regularizers in 1 sufficiently small. By following the same analysis, we can achieve the same convergence results as with the  $\ell_p$  regularization problem.

Table 1: Examples of regularized functions and weight expressions

Regularizer	$r( \mathbf{x} )$	$[\omega(\mathbf{x})]_i = r'( x_i )$	$r''( x_i )$
LPN [2]	$\sum_{i=1}^n ( x_i )^q$	$q( x_i )^{q-1}$	$q(q-1)( x_i )^{q-2}$
LOG [46]	$\sum_{i=1}^n \log(1 + \frac{ x_i }{q})$ ,	$\frac{1}{ x_i +q}$	$-\frac{1}{( x_i +q)^2}$
FRA [2]	$\sum_{i=1}^n \frac{ x_i }{ x_i +q}$	$\frac{q}{( x_i +q)^2}$	$-\frac{2q}{( x_i +q)^3}$
TAN [10]	$\sum_{i=1}^n \arctan(\frac{ x_i }{q})$	$\frac{q}{q^2 + ( x_i )^2}$	$\frac{-2q x_i }{(q^2 +  x_i ^2)^2}$
EXP [47]	$\sum_{i=1}^n 1 - e^{-\frac{ x_i }{q}}$	$\frac{1}{q} e^{-\frac{ x_i }{q}}$	$-\frac{1}{q^2} e^{-\frac{ x_i }{q}}$

## 6 Numerical results

In this section, we present our method for the  $\ell_p$ -norm regularized logistic regression problem, defined as follows,

$$\underset{\mathbf{x} \in \mathbb{R}^n}{\text{minimize}} \quad \sum_{i=1}^m \log(1 + e^{-a_i \mathbf{x}^T \mathbf{b}_i}) + \lambda \|\mathbf{x}\|_p^p,$$

where  $m$  is the number of feature vectors,  $a_i \in \{-1, 1\}$ ,  $\mathbf{b}_i \in \mathbb{R}^n$ ,  $i = 1, \dots, m$  are the labels and feature vectors respectively. This problem has broad applications in various fields, including image classification and natural language processing (NLP).

In the test, we use SOIR $\ell_1$  on some datasets to demonstrate its local convergence behavior. Additionally, we apply SOIR $\ell_1$  to an array of real-world datasets for comparative analysis against other state-of-the-art methods. All codes are implemented in MATLAB and run on a PC with an i9-13900K 3.00 GHz CPU and 64GB RAM. We test our method on a synthetic dataset and 6 real-world datasets. The synthetic dataset is generated following [37, 48]. The labels  $a_i$  are drawn from  $\{-1, +1\}$  using Bernoulli distribution. The feature matrix  $B = [b_1, \dots, b_m]^\top$  is drawn from a standard Gaussian distribution, with minor adjustments to ensure symmetry. The real-world datasets are binary classification examples collected from the LIBSVM repository, including *w8a*, *a9a*, *real-sim*, *gisette*, *news20* and *rcv1.train*. All datasets have a sufficiently large feature size appropriate for a sparsity-driven problem.

We compare the performance of SOIR $\ell_1$  with HpgSRN[36] which is a hybrid Newton method with Q-superlinear optimal convergence rate and EPIR $\ell_1$  [15] which is an iteratively reweighted  $\ell_1$  first-order method. Both methods are the most recent algorithms tailored for Problem  $\mathcal{P}$ . For all experiments, we follow the original settings for HpgSRN and EPIR $\ell_1$  and use the same termination condition to ensure fairness. For all methods, the initial point  $\mathbf{x}^0$  is set as the zero vector.

### 6.1 Implementation details

In Algorithm 1, we generally choose for the fixed parameters

$$\gamma = 1, \eta_\Phi = 1, \eta_\Psi = 1, \tau = 10^{-8}, \alpha = 10^{-8}, \xi = 0.5, \varpi = 0.1.$$

For line 16–18 in Algorithm 1, we choose the Conjugate Gradient (CG) method to solve the reduced space quadratic programming problem. Initially, we run the CG method with  $\zeta = 0$ ; if no descent direction is found, we choose a  $\zeta = 10^{-8} + 10^{-4} \|\nabla_{\mathcal{W}_k} F(\mathbf{x}^k; \boldsymbol{\epsilon}^k)\|^{0.5} + \delta^k$  where  $\delta^k = \min\{\lambda p(p-1) |x_i^k|^{p-2} \mid i \in \mathcal{I}(\mathbf{x}^k)\}$  large enough to make  $\nabla_{\mathcal{W}_k}^2 F(\mathbf{x}^k; \boldsymbol{\epsilon}^k)$  positive definite. Since the termination condition in line 18 is always satisfied during the CG method, we applied a truncated CG method described in [37, Section 4.2]. For the alternative choice in 5.1, we follow the parameters set in [45]. For line 11 and line 14 in Algorithm 1, while the descent direction is based solely on gradient information, proper scaling for the initial stepsize  $\bar{\mu}$  is necessary in a practical approach. We choose the stepsize using the Barzilai-Borwein (BB) rule [49]. Such scaling has no influence on the whole theory we developed.

The  $\epsilon$  update strategy significantly impacts various facets of our algorithm. Utilizing a mild update strategy likely enlarges  $|\mathcal{S}_\Psi|$ , thereby enhancing the likelihood of identifying a better active manifold. Conversely, this approach may prolong the minimization on the perturbed objective function when  $\epsilon$  is insufficiently small, consequently increasing computational time. An illustrative experiment on the synthetic dataset with feature dimensions  $m = 1000$  and  $n = 1000$  is shown in Table 2. Being fully aware of such properties, we carefully set the  $\epsilon$  update

Table 2: Simple demonstration on  $\epsilon$  update strategy.

$\beta$	0.01	0.3	0.5	0.7	0.9	0.99
Time	0.05	0.15	0.16	0.19	0.19	0.26
Objective	579.14	534.52	506.12	495.85	495.07	493.96
Sparsity	87.10%	72.80%	62.50%	61.60%	61.70%	61.00%

strategy for line 25 as follows,

$$\epsilon_i^{k+1} = \begin{cases} 0.9\epsilon_i^k, & k \in \mathcal{S}_\Psi, i \in \mathcal{I}^{k+1}, \\ 0.9(\epsilon_i^k)^{1.1}, & k \in \mathcal{S}_\Phi, i \in \mathcal{I}^{k+1}, \\ \min\{0.9\epsilon_i^k, (\epsilon_i^k)^2\}, & k \in \mathcal{S}_{QP}, i \in \mathcal{I}^{k+1}, \\ \epsilon_i^k, & \text{otherwise.} \end{cases}$$

with  $\epsilon^0 = 1$ . For  $k \in \mathcal{S}_\Phi$ , we specifically use  $0.9(\epsilon_i^k)^{1.1} \leq 0.9\epsilon_i^k$  to accelerate the convergence of  $\epsilon$ . An additional lower bound for  $\epsilon_i^k$  is added before any local problem is triggered, that is  $\epsilon_i^k = \max\{\epsilon_i^k, 10^{-8}\}$  if  $[k] \in \mathcal{S}_\Psi \cup \mathcal{S}_\Phi$ . This bound allows the algorithm to smooth out suboptimal local points.

## 6.2 Numerical Results

### 6.2.1 Local quadratic convergence

We first apply SOIR $\ell_1$  to the synthetic dataset and the six real-world datasets with  $\lambda = 1$  to demonstrate the local convergence behavior. In addition to the parameter configurations specified in section 6.1, we remove the termination condition in the CG method to ensure the local Newton step is fully executed. We evaluate the local convergence behavior through the examination of the optimal residual  $\mathcal{R}_{opt}$  and the distance residual  $\mathcal{R}_{dist}$ .

$$\mathcal{R}_{opt} = \|\mathbf{x} \nabla f(\mathbf{x}) + \lambda p|\mathbf{x}|^p\|_\infty, \quad \mathcal{R}_{dist} = \|\mathbf{x} - \mathbf{x}^*\|_\infty.$$

We plot the logarithm of  $\mathcal{R}_{opt}$  and  $\mathcal{R}_{dist}$  for the final ten iterations from each dataset, as shown in Figure 1. Panels (a) and (b) depict  $\log_{10}(\mathcal{R}_{opt})$  and  $\log_{10}(\mathcal{R}_{dist})$  over the last ten iterations across six real-world datasets. Panels (c) and (d) depict the same metrics against the last ten iterations on synthetic datasets. Two scales with dimensions  $m, n = 500$  and  $m, n = 2000$  were selected for synthetic data. For each scale, 20 random trials were conducted, with the average displayed in bold. The local quadratic convergence can be witnessed by the scope, with most curve less than  $-2$ .

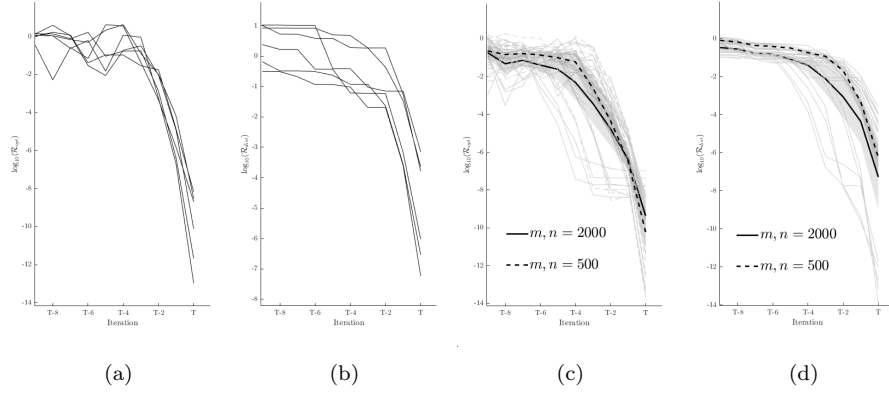


Fig. 1: Local quadratic convergence behavior on real-world and synthetic datasets.

### 6.2.2 Real world datasets with $p = 0.5$

Then we compare SOIR $\ell_1$  to the hybrid Newton method HpgSRN and the iteratively reweighted first-order method EPIR $\ell_1$  on real-world datasets. We use SOIR $\ell_1$ -MN to denote the original Algorithm 1 and SOIR $\ell_1$ -TR denotes the alternative local subproblem method discussed in section 5.1. Initially, we standardize parameters across all datasets, setting  $\lambda = 1$  and  $p = 0.5$ . Our primary focus is on evaluating performance based on CPU time, objective value, and the percentage of zeros. To ensure accuracy, we repeat all experiments 10 times, taking the average of these values. For the second-order methods HpgSRN and SOIR $\ell_1$ , the algorithm is terminated when  $\mathcal{R}_{opt}$  decreases to  $10^{-8}$  and  $\|\mathbf{x}^k - \mathbf{x}^{k-1}\|/\|\mathbf{x}^k\| < 10^{-9}$  (which is a straight inference for optimality measurement based on lemma 2 and lemma 5). For EPIR $\ell_1$ , considering the trailing effect of first-order methods, we maintain its original termination condition of  $\|\mathbf{x}^k - \mathbf{x}^{k-1}\|/\|\mathbf{x}^k\| < 10^{-4}$  in addition to  $\mathcal{R}_{opt}$ . We limit EPIR $\ell_1$  to a maximum of 5000 iterations and all methods to a maximum time of 500 seconds. The performance of the three methods is shown in Table 3, with the best performance among the three methods highlighted in bold. Here we summarize the performance:

- (i) In general, the second-order methods (SOIR $\ell_1$ -MN, SOIR $\ell_1$ -TR, HpgSRN) perform better than the first-order method (EPIR $\ell_1$ ) in terms of CPU time. SOIR $\ell_1$ -TR requires the least CPU time on *gisette* and *a9a* while SOIR $\ell_1$ -MN requires least on the rest. Compared to HpgSRN, our method consistently shows a marked advantage in computational speed.
- (ii) Our methods (SOIR $\ell_1$ -MN, SOIR $\ell_1$ -TR) always achieve the lowest or near-lowest objective values, suggesting effectiveness in minimizing the logistic regression problem. In some cases (e.g., *w8a*), while SOIR $\ell_1$  does not always achieve the absolute best objective value, it remains competitive with other algorithms.
- (iii) While maintaining low objective values, our methods (SOIR $\ell_1$ -MN, SOIR $\ell_1$ -TR) also maintain a sparsity similar to or better than the baseline (e.g., *gisette*).

Overall, our methods exhibit outstanding time efficiency across all datasets, often by significant margins, and solve with superior objective function values and competitive sparsity.

Table 3: Performance comparison on real-world datasets with  $p = 0.5$ . The size of the feature matrix is enclosed in parentheses.

dataset	Algorithm	Time (s)	Objective	% of zeros
a9a (32561×123)	SOIR $\ell_1$ -MN	0.5007	10579.4	45.53%
	SOIR $\ell_1$ -TR	<b>0.4194</b>	10588.5	46.34%
	HpgSRN	2.9001	10583.3	<b>53.01%</b>
	EPIR $\ell_1$	5.9884	<b>10570.5</b>	39.02%
w8a (49749×300)	SOIR $\ell_1$ -MN	<b>0.6145</b>	5873.8	37.00%
	SOIR $\ell_1$ -TR	1.3807	5876.9	37.00%
	HpgSRN	2.0102	<b>5856.5</b>	37.00%
	EPIR $\ell_1$	13.0460	5865.1	<b>38.00%</b>
gisette (6000×5000)	SOIR $\ell_1$ -MN	35.0693	176.4	97.06%
	SOIR $\ell_1$ -TR	<b>32.7069</b>	<b>176.2</b>	<b>97.06%</b>
	HpgSRN	36.5831	177.0	96.92%
	EPIR $\ell_1$	326.4776	178.3	97.02%
real sim (72309×20958)	SOIR $\ell_1$ -MN	<b>3.8057</b>	<b>7121.6</b>	93.63%
	SOIR $\ell_1$ -TR	10.0057	7123.3	93.63%
	HpgSRN	6.8014	7262.3	<b>94.47%</b>
	EPIR $\ell_1$	33.4761	7152.7	93.78%
rcv1.train (20242×47236)	SOIR $\ell_1$ -MN	<b>1.5928</b>	<b>2554.6</b>	99.10%
	SOIR $\ell_1$ -TR	3.9464	2558.9	99.08%
	HpgSRN	1.6934	2578.4	<b>99.21%</b>
	EPIR $\ell_1$	14.0964	2562.9	99.13%
news20 (19996×1355191)	SOIR $\ell_1$ -MN	<b>20.0840</b>	4034.5	99.97%
	SOIR $\ell_1$ -TR	93.5413	3989.7	99.97%
	HpgSRN	23.7392	4171.3	<b>99.97%</b>
	EPIR $\ell_1$	207.0546	<b>3983.6</b>	99.97%

### 6.3 General nonconvex regularizers

#### 6.3.1 Different $p$ value

The regularization problem with a small  $\ell_p$ -norm presents a more challenging task due to its stronger nonconvexity, compared to cases with larger  $p$  values. To demonstrate our method's superior performance, we conduct tests with  $p = 0.3$  on SOIR $\ell_1$ -MN and HpgSRN for comparison. The problem settings and algorithm configurations were otherwise kept consistent.

For a clearer presentation of our findings, we have summarized the CPU times and objective values in Table 4. The results demonstrate that SOIR $\ell_1$ -MN significantly outperforms HpgSRN, particularly when compared with the performance under the  $p = 0.3$  scenario. This advantage is more pronounced on datasets with large feature sizes, such as *real-sim* and *news20*. For these datasets, HpgSRN's CPU time increases substantially—by factors of 7 and 78, respectively—while the

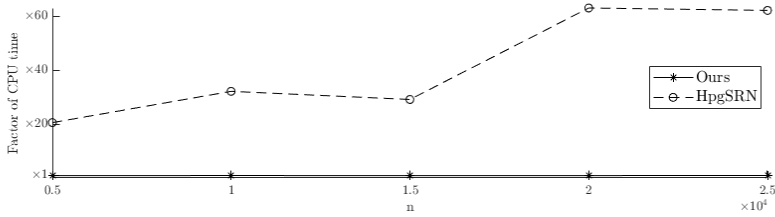


Fig. 2: Comparison against HpgSRN with  $p = 0.3$  on synthetic datasets. The synthetic datasets were generated with  $m = 5000$  and varying  $n$  values ranging from 5000 to 25000. The  $y$ -axis represents the factor of CPU times, comparing the time for  $p = 0.3$  to the time for  $p = 0.5$ .

CPU time for our method remains stable, similar to that observed in the  $p = 0.5$  scenario. A direct comparison on synthetic datasets is illustrated in Figure 2. As the feature size increases, our method demonstrates minimal increases in CPU time, in stark contrast to HpgSRN, whose CPU time increases at a dizzying rate.

The reasons for this can be summarized as follows: (i) There is no analytical solution for the proximal mapping except for  $p = 0.5$  and  $p = 2/3$ , so HpgSRN applies a numerical method for  $p = 0.3$  on the entire index set  $\mathbb{R}^n$ , while we only perform a soft thresholding step on a subset defined in line 13 or 10. (ii) From 2, we show that our method has a zero components detection scheme based on the  $\epsilon$  update strategy, which can quickly discard bad indices and force the method to enter the local phase.

Table 4: Comparison against HpgSRN with  $p = 0.3$  on real-world datasets.

	Dataset	news20	w8a	a9a	real sim	rcv1.train	gisette
SOIR $\ell_1$ -MN	Time (s)	60.21	0.80	0.47	9.01	3.86	31.79
	Objective	3019.06	5825.87	10596.93	5669.32	1933.62	165.18
HpgSRN	Time (s)	1871.86	3.29	3.49	50.67	15.73	34.07
	Objective	3696.13	5802.88	10595.47	6099.26	2078.87	186.27

### 6.3.2 Four different regularizers

To evaluate Algorithm 1 on a generic nonconvex regularization problem, we apply all regularizers listed in 1 to the logistic regression problem. We utilize the datasets *a9a*, *gisette*, and *rcv1.train*, which each have a number of features on three distinct scales, as illustrative examples. To promote sparsity, we set  $\lambda = 1$  and use different values of  $q$  for different regularizations. The performance is depicted in Figure 3, where we plot the logarithmic residuals across the last 10 iterations. The residual is defined as

$$\mathcal{R}_{opt} = \|\mathbf{x} \circ (\nabla f(\mathbf{x}) + \boldsymbol{\omega}(\mathbf{x}, \mathbf{0}) \circ \text{sgn}(\mathbf{x}))\|_\infty.$$

which serves as an indicator of the stationarity condition. Based on the data presented in Figure 3, it is evident that most regularizers successfully converge to a level of  $10^{-8}$ .

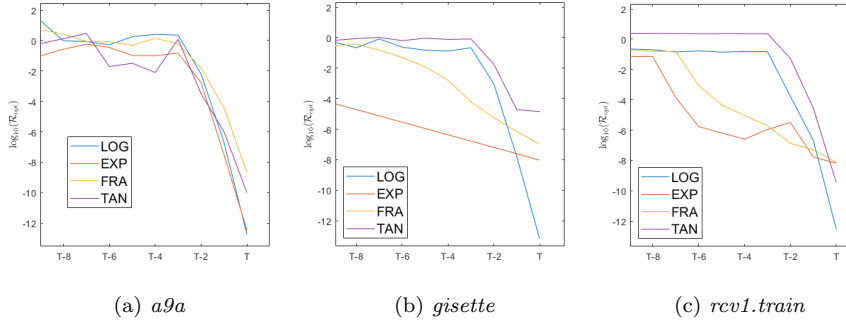


Fig. 3: Convergence result for four different regularizers on three real-world datasets. To ensure Assumption 8, we set  $q = 10^{-5}$  for LOG regularizer and  $q = 0.1$  for others.

## Conclusion

In this paper, we introduce a second-order iteratively reweighted  $\ell_1$  method for a class of nonconvex sparsity-promoting regularization problems. Our approach, by reformulating nonconvex regularization into weighted  $\ell_1$  form and incorporating subspace approximate Newton steps with subspace soft-thresholding steps, not only speeds up computation but also ensures algorithmic stability and convergence.

We prove global convergence under Lipschitz continuity and bounded Hessian conditions, achieving local superlinear convergence under KL property framework and local quadratic convergence with a strategic perturbation update. The method also extends to nonconvex and nonsmooth sparsity-driven regularization problems, maintaining similar convergence results. Empirical tests across various model prediction scenarios have demonstrated the method's efficiency and effectiveness, suggesting its utility for complex optimization challenges in sparsity and nonconvexity contexts.

## Acknowledgments

We would like to acknowledge the support for this paper from the Young Scientists Fund of the National Natural Science Foundation of China No. 12301398.

## Appendix

**Lemma 7** *Let  $d(\mu) = \mathcal{S}_{\mu\omega}(\mathbf{x} - \mu\mathbf{g}) - \mathbf{x}$  for  $\mu > 0$  where  $\mathbf{x}, \mathbf{g} \in \mathbb{R}^n$  and  $\omega \in \mathbb{R}_{++}^n$ . It holds that*

$$d_i(\mu) = \mu d_i(1) \quad \text{if } x_i = 0, \quad (1)$$

$$|d_i(\mu)| \geq \min\{\mu, 1\} |d_i(1)| \quad \text{if } x_i \neq 0. \quad (2)$$

Moreover, for  $\omega_i > |g_i - x_i|$ ,  $d_i(\mu) = -x_i$ .

*Proof* It holds from the soft-thresholding operator that

$$d_i(\mu) = \begin{cases} -\mu(g_i + \omega_i), & \text{if } \mu(g_i + \omega_i) < x_i, \\ -\mu(g_i - \omega_i), & \text{if } \mu(g_i - \omega_i) > x_i, \\ -x_i, & \text{otherwise.} \end{cases} \quad (3)$$

If  $i \in \mathcal{I}_0(\mathbf{x})$ ,  $x_i = 0$ . It is obvious that  $d_i(\mu) = -\mu d_i(1)$ .

If  $i \in \mathcal{I}(\mathbf{x})$ ,  $x_i \neq 0$ . We check the values of  $d_i(1)$ .

If  $d_i(1) = -(g_i + \omega_i)$ , which means

$$g_i + \omega_i < x_i \quad (4)$$

by the expression of  $d_i(1)$ , we consider the order of  $x_i, \mu(g_i + \omega_i), \mu(g_i - \omega_i)$ .

Case (a):  $\mu(g_i - \omega_i) < \mu(g_i + \omega_i) < x_i$ , this belongs to the first case in  $d_i(\mu)$ , meaning  $d_i(\mu) = -\mu d_i(1)$ .

Case (b):  $\mu(g_i - \omega_i) \leq x_i \leq \mu(g_i + \omega_i)$ , this belongs to the third case in  $d_i(\mu)$ , so that  $d_i(\mu) = -x_i$ . It follows from (4) that

$$g_i + \omega_i < x_i < \mu(g_i + \omega_i), \quad (5)$$

meaning  $0 < g_i + \omega_i < x_i, \mu > x_i/(g_i + \omega_i) > 1$  or  $g_i + \omega_i < x_i < 0, \mu < x_i/(g_i + \omega_i) < 1$  by noticing (4). In either case,  $|x_i| > \min(\mu, 1)|g_i + \omega_i|$ , meaning  $|d_i(\mu)| > \min(\mu, 1)|d_i(1)|$ .

Case (c):  $x_i < \mu(g_i - \omega_i) < \mu(g_i + \omega_i)$ , this belongs to the second case in  $d_i(\mu)$ , so that  $d_i(\mu) = -\mu(g_i - \omega_i)$ . It follows from (4) that

$$g_i + \omega_i < \mu(g_i - \omega_i) < \mu(g_i + \omega_i), \quad (6)$$

meaning  $\nabla_i f(\mathbf{x}) + \omega_i > 0, \mu > 1$  or  $\nabla_i f(\mathbf{x}) + \omega_i < 0, \mu < 1$ . In either case, (6) implies that  $|\mu(g_i - \omega_i)| > \min(\mu, 1)|g_i + \omega_i|$ , indicating  $|d_i(\mu)| > \min(\mu, 1)|d_i(1)|$ .

If  $d_i(1) = -(g_i - \omega_i)$ , this means  $g_i + \omega_i < x_i$ . same argument based on the order of we consider the order of  $x_i, \mu(g_i + \omega_i), \mu(g_i - \omega_i)$  also yields (2)

If  $d_i(1) = -x_i$ , this means  $g_i + \omega_i > x_i > g_i - \omega_i$ , the same argument based on the order of we consider the order of  $x_i, \mu(g_i + \omega_i), \mu(g_i - \omega_i)$  also yields (2).

## References

1. R Tyrrell Rockafellar and Roger J-B Wets. *Variational Analysis*, volume 317. Springer Berlin, Heidelberg, Germany, 2009.
2. Maryam Fazel, Haitham Hindi, and Stephen P Boyd. Log-det heuristic for matrix rank minimization with applications to hankel and euclidean distance matrices. In *Proceedings of the 2003 American Control Conference*, volume 3, pages 2156–2162. IEEE, 2003.
3. Jianqing Fan and Runze Li. Variable selection via nonconcave penalized likelihood and its oracle properties. *Journal of the American Statistical Association*, 96(456):1348–1360, 2001.
4. Cun-Hui Zhang. Nearly unbiased variable selection under minimax concave penalty. *The Annals of Statistics*, 38(2):894–942, 2010.
5. Tong Zhang. Analysis of multi-stage convex relaxation for sparse regularization. *Journal of Machine Learning Research*, 11(3), 2010.
6. Rick Chartrand. Exact reconstruction of sparse signals via nonconvex minimization. *IEEE Signal Processing Letters*, 14(10):707–710, 2007.

7. Silvia Gazzola, James G Nagy, and Malena Sabate Landman. Iteratively reweighted fgmres and flsqr for sparse reconstruction. *SIAM Journal on Scientific Computing*, 43(5):S47–S69, 2021.
8. Xiong Zhou, Xianming Liu, Chenyang Wang, Deming Zhai, Junjun Jiang, and Xiangyang Ji. Learning with noisy labels via sparse regularization. In *Proceedings of the IEEE/CVF International Conference on Computer Vision*, pages 72–81, 2021.
9. Zhenqiu Liu, Feng Jiang, Guoliang Tian, Suna Wang, Fumiaki Sato, Stephen J Meltzer, and Ming Tan. Sparse logistic regression with lp penalty for biomarker identification. *Statistical Applications in Genetics and Molecular Biology*, 6(1), 2007.
10. Emmanuel J Candes, Michael B Wakin, and Stephen P Boyd. Enhancing sparsity by reweighted  $\ell_1$  minimization. *Journal of Fourier Analysis and Applications*, 14:877–905, 2008.
11. Yaohua Hu, Chong Li, Kaiwen Meng, Jing Qin, and Xiaoqi Yang. Group sparse optimization via  $\ell_{p,q}$  regularization. *The Journal of Machine Learning Research*, 18(1):960–1011, 2017.
12. Zhaosong Lu. Iterative reweighted minimization methods for  $\ell_p$  regularized unconstrained nonlinear programming. *Mathematical Programming*, 147(1-2):277–307, 2014.
13. Hao Wang, Hao Zeng, Jiashan Wang, and Qiong Wu. Relating  $\ell_p$  regularization and reweighted  $\ell_1$  regularization. *Optimization Letters*, 15(8):2639–2660, 2021.
14. Hao Wang, Hao Zeng, and Jiashan Wang. Convergence rate analysis of proximal iteratively reweighted  $\ell_1$  methods for  $\ell_p$  regularization problems. *Optimization Letters*, 17(2):413–435, 2023.
15. Hao Wang, Hao Zeng, and Jiashan Wang. An extrapolated iteratively reweighted  $\ell_1$  method with complexity analysis. *Computational Optimization and Applications*, 83(3):967–997, 2022.
16. Ming-Jun Lai, Yangyang Xu, and Wotao Yin. Improved iteratively reweighted least squares for unconstrained smoothed  $\ell_q$  minimization. *SIAM Journal on Numerical Analysis*, 51(2):927–957, 2013.
17. Xiaojun Chen, Lingfeng Niu, and Yaxiang Yuan. Optimality conditions and a smoothing trust region newton method for non-Lipschitz optimization. *SIAM Journal on Optimization*, 23(3):1528–1552, 2013.
18. Xiaojun Chen and Weijun Zhou. Convergence of the reweighted  $\ell_1$  minimization algorithm for  $\ell_2 - \ell_p$  minimization. *Computational Optimization and Applications*, 59(1-2):47–61, 2014.
19. Xiaojun Chen and Weijun Zhou. Convergence of reweighted  $\ell_1$  minimization algorithms and unique solution of truncated  $\ell_p$  minimization. *Department of Applied Mathematics, The Hong Kong Polytechnic University*, 2010.
20. Zongben Xu, Xiangyu Chang, Fengmin Xu, and Hai Zhang.  $l_{1/2}$  regularization: A thresholding representation theory and a fast solver. *IEEE Transactions on Neural Networks and Learning Systems*, 23(7):1013–1027, 2012.
21. Ming-Jun Lai and Jingyue Wang. An unconstrained  $\ell_q$  minimization with  $0 < q \leq 1$  for sparse solution of underdetermined linear systems. *SIAM Journal on Optimization*, 21(1):82–101, 2011.
22. Peiran Yu and Ting Kei Pong. Iteratively reweighted  $\ell_1$  algorithms with extrapolation. *Computational Optimization and Applications*, 73(2):353–386, 2019.
23. Feishe Chen, Lixin Shen, and Bruce W Suter. Computing the proximity operator of the  $\ell_p$  norm with  $0 < p < 1$ . *IET Signal Processing*, 10(5):557–565, 2016.
24. Yulan Liu and Rongrong Lin. A bisection method for computing the proximal operator of the  $\ell_p$ -norm for any  $0 < p < 1$  with application to schatten p-norms. *Journal of Computational and Applied Mathematics*, 447:115897, 2024.
25. Yaohua Hu, Chong Li, Kaiwen Meng, and Xiaoqi Yang. Linear convergence of inexact descent method and inexact proximal gradient algorithms for lower-order regularization problems. *Journal of Global Optimization*, 79(4):853–883, 2021.
26. Jason D Lee, Yuekai Sun, and Michael A Saunders. Proximal newton-type methods for minimizing composite functions. *SIAM Journal on Optimization*, 24(3):1420–1443, 2014.
27. Man-Chung Yue, Zirui Zhou, and Anthony Man-Cho So. A family of inexact sqa methods for non-smooth convex minimization with provable convergence guarantees based on the luo-tseng error bound property. *Mathematical Programming*, 174(1):327–358, 2019.
28. Boris S Mordukhovich, Xiaoming Yuan, Shangzhi Zeng, and Jin Zhang. A globally convergent proximal newton-type method in nonsmooth convex optimization. *Mathematical Programming*, 198(1):899–936, 2023.

29. Ruyu Liu, Shaohua Pan, Yuqia Wu, and Xiaoqi Yang. An inexact regularized proximal newton method for nonconvex and nonsmooth optimization. *Computational Optimization and Applications*, pages 1–39, 2024.
30. James V Burke and Jorge J Moré. On the identification of active constraints. *SIAM Journal on Numerical Analysis*, 25(5):1197–1211, 1988.
31. Jingwei Liang, Jalal Fadili, and Gabriel Peyré. Activity identification and local linear convergence of forward–backward-type methods. *SIAM Journal on Optimization*, 27(1):408–437, 2017.
32. Yifan Sun, Halyun Jeong, Julie Nutini, and Mark Schmidt. Are we there yet? manifold identification of gradient-related proximal methods. In *The 22nd International Conference on Artificial Intelligence and Statistics*, pages 1110–1119. PMLR, 2019.
33. Andreas Themelis, Lorenzo Stella, and Panagiotis Patrinos. Forward-backward envelope for the sum of two nonconvex functions: Further properties and nonmonotone linesearch algorithms. *SIAM Journal on Optimization*, 28(3):2274–2303, 2018.
34. Andreas Themelis, Masoud Ahookhosh, and Panagiotis Patrinos. On the acceleration of forward-backward splitting via an inexact newton method. *Splitting Algorithms, Modern Operator Theory, and Applications*, pages 363–412, 2019.
35. Gilles Bartheilles, Franck Iutzeler, and Jérôme Malick. Newton acceleration on manifolds identified by proximal gradient methods. *Mathematical Programming*, 200(1):37–70, 2023.
36. Yuqia Wu, Shaohua Pan, and Xiaoqi Yang. A regularized Newton method for  $\ell_q$ -norm composite optimization problems. *SIAM Journal on Optimization*, 33(3):1676–1706, 2023.
37. Tianyi Chen, Frank E Curtis, and Daniel P Robinson. A reduced-space algorithm for minimizing  $\ell_1$ -regularized convex functions. *SIAM Journal on Optimization*, 27(3):1583–1610, 2017.
38. Hedy Attouch, Jérôme Bolte, and Benar Fux Svaiter. Convergence of descent methods for semi-algebraic and tame problems: proximal algorithms, forward–backward splitting, and regularized Gauss–Seidel methods. *Mathematical Programming*, 137(1-2):91–129, 2013.
39. Jérôme Bolte, Shoham Sabach, and Marc Teboulle. Proximal alternating linearized minimization for nonconvex and nonsmooth problems. *Mathematical Programming*, 146(1):459–494, 2014.
40. Zhi-Quan Luo, Jong-Shi Pang, and Daniel Ralph. *Mathematical programs with equilibrium constraints*. Cambridge University Press, Cambridge, 1996.
41. Jinshan Zeng, Shaobo Lin, and Zongben Xu. Sparse regularization: Convergence of iterative jumping thresholding algorithm. *IEEE Transactions on Signal Processing*, 64(19):5106–5118, 2016.
42. Guoyin Li and Ting Kei Pong. Calculus of the exponent of kurdyka–łojasiewicz inequality and its applications to linear convergence of first-order methods. *Foundations of Computational Mathematics*, 18(5):1199–1232, 2018.
43. Hedy Attouch and Jérôme Bolte. On the convergence of the proximal algorithm for nonsmooth functions involving analytic features. *Mathematical Programming*, 116:5–16, 2009.
44. Bo Wen, Xiaojun Chen, and Ting Kei Pong. A proximal difference-of-convex algorithm with extrapolation. *Computational optimization and applications*, 69(2):297–324, 2018.
45. Frank E Curtis, Daniel P Robinson, Clément W Royer, and Stephen J Wright. Trust-region newton-cg with strong second-order complexity guarantees for nonconvex optimization. *SIAM Journal on Optimization*, 31(1):518–544, 2021.
46. Miguel Sousa Lobo, Maryam Fazel, and Stephen Boyd. Portfolio optimization with linear and fixed transaction costs. *Annals of Operations Research*, 152:341–365, 2007.
47. Paul S Bradley, Olvi L Mangasarian, and W Nick Street. Feature selection via mathematical programming. *INFORMS Journal on Computing*, 10(2):209–217, 1998.
48. N Keskar, Jorge Nocedal, Figen Öztoprak, and Andreas Waechter. A second-order method for convex 1-regularized optimization with active-set prediction. *Optimization Methods and Software*, 31(3):605–621, 2016.
49. Jonathan Barzilai and Jonathan M Borwein. Two-point step size gradient methods. *IMA journal of numerical analysis*, 8(1):141–148, 1988.